Development of an Agent-Based Model of Long-term Disease Progression in Duchenne Muscular Dystrophy

---

A Thesis

Presented to

the faculty of the School of Engineering and Applied Science

University of Virginia

---

in partial fulfillment

of the requirements for the degree

Master of Science

by

Katherine B. Crump

May 2021

APPROVAL SHEET

This Thesis

is submitted in partial fulfillment of the requirements

for the degree of

Master of Science

Author Signature: _____

This Thesis has been read and approved by the examining committee:

Advisor: _____

Advisor: _____

Committee Member: _____

Committee Member: _____

Committee Member: _____

Committee Member: _____

Accepted for the School of Engineering and Applied Science:

Craig H. Benson, School of Engineering and Applied Science

May 2021

Abstract

Duchenne muscular dystrophy (DMD) is a severe muscle wasting disease that affects 1 in every 3,500 boys. Patients with DMD require a wheelchair by age 12, and ultimately die due to respiratory or cardiac failure by the mid 20s. The initiating cause of DMD is known – the absence of dystrophin, a protein that associates with a multimolecular network of integral and subsarcolemmal proteins, known as the dystrophin glycoprotein complex (DGC). Dystrophin and the DGC form a physical link between the intracellular cytoskeleton of the muscle fiber and the extracellular matrix. Without dystrophin, the DGC fails to properly form at the sarcolemma and the link is compromised, which diminishes the strength of the muscle fiber membrane. The weak membrane is susceptible to damage by muscle contractions during everyday movements, which can initiate a cascade of muscle fiber necrosis, chronic inflammation, and ultimately progressing to severe muscle weakness. However, despite extensive research and knowing the cause of DMD, there is no cure for DMD and current treatments have had limited efficacy because promising treatments in mice do not translate to clinical benefit in patients. Treatment is difficult because DMD and muscle regeneration are complex processes, involving mechanisms that transcend spatial and temporal scales.

Computational modeling provides a powerful to tool to investigate complex behaviors in skeletal muscle that may not be accessible through experiments due to cost or limitations in equipment. In this thesis, I present a computational model of chronic muscle degeneration in the *mdx* mouse. Through modifications to an acute injury model of DMD published by Virgilio et al., the new model presented here combines the strengths of other previously developed

computational models (Martin et al., Jarrah et al., and Houston et al.) to offer a more comprehensive simulation of repetitive injury, cellular interactions, inflammatory cues, and muscle repair. New dystrophic conditions were defined by literature-derived rules and various damage protocols were tested to produce a model of disease progression in the *mdx* mouse that is validated by published literature data on change in fibrosis, satellite stem cell count, and macrophage cell count. Through low-level, daily injuries, the model simulations capture the peak damage before the *mdx* mouse is 3 months old and the switch from a pro-inflammatory environment to an anti-inflammatory, pro-fibrotic environment after 6 months.

Acknowledgements

Returning to UVA for graduate school has been an incredible and rewarding learning experience. Navigating graduate school would not have been successful without such an amazing, supportive network of mentors, colleagues, friends, and family.

First, I must acknowledge my mentors Silvia Blemker and Shayn Peirce-Cottler. Silvia has been an amazing mentor for me since my 2nd year of undergrad in 2015, starting with research on the biomechanics of yoga, then working at Springbok, and now in my Masters. Both Silvia and Shayn have been an endless source of inspiration, and their excitement for science is contagious. Co-mentorship is not a common path, but the combined mentorship of Shayn and Silvia was perfect for guiding me and my project; their expertise truly complemented each other and led to interesting weekly discussions that always left me excited to learn more. Additionally, navigating grad school through a pandemic has not been easy, and I appreciate the tremendous amount of encouragement that they provided throughout and the amount of support they gave when I decided my next steps. I could not have asked for better examples of women navigating STEM and academic careers, and I hope that I can be as good a mentor to young female scientists one day as they were for me.

I was also lucky to be able to work with a clinician, Dr. Rebecca Sharf, on my committee, and have benefitted from her insights into DMD. The connection to the DMD clinic through Rebecca helped to really understand how my research is helping patients and why it is important.

I would also like to thank both the current and former members of the Multiscale Muscle Mechanophysiology Lab and the Peirce-Cottler Lab for their support and insight. I have appreciated the puns, wing days, happy hours (virtual and in person!), coffee runs, and

continuous encouragement from all of you. It was amazing to have such great lab mates to help answer my Repast and science questions, troubleshoot code that isn't working, and provide feedback on grants and presentations. And thank you to Anthony for answering my endless questions on histology. I would also like to thank Kyle Martin and Kelley Virgilio for helping me get started in the muscle regeneration ABM and for paving the way. I also appreciate my BME cohort, especially Allie, Julie, and Tor for the endless support these past two years and for making grad school a more fun experience, even when half of it was remote.

Although they may not understand exactly what I'm doing, my family has been an incredible source of support for the past two years and throughout my life. I also could not have done this without Pablo; even all the way in Europe, he was there to help me get through a crazy, difficult year.

I have learned a lot these past two years, and truly appreciate this opportunity that I have had to become a double hoo and all the support from everyone who helped me on this journey.

Table of Contents

List of Figures

List of Tables

Chapter 1 : Introduction

Skeletal muscle is a highly dynamic and plastic tissue that drives movement in our daily life [1]. It is essential for breathing, walking, communicating, physical activity; and the loss of skeletal muscle function can lead to disability and impair quality of life. Duchenne Muscular Dystrophy (DMD) is a severe muscle wasting disease caused by the lack of dystrophin, a skeletal muscle protein that protects muscle fibers against contraction-induced damage [2]. Due to the lack of dystrophin, dystrophic muscles are very easily damaged during normal daily use, yielding chronic inflammation, muscle fiber necrosis, satellite cell depletion, fibrosis, and fatty infiltration [3,4]. Treatments are merely palliative, as there is no cure for the disease. Patients who suffer from DMD will be affected starting around the age of 5, leaving them using a wheelchair for mobility as a teenager, and ultimately they may not live past their 20s due to respiratory failure or cardiomyopathy [5] (Fig. 1.1).

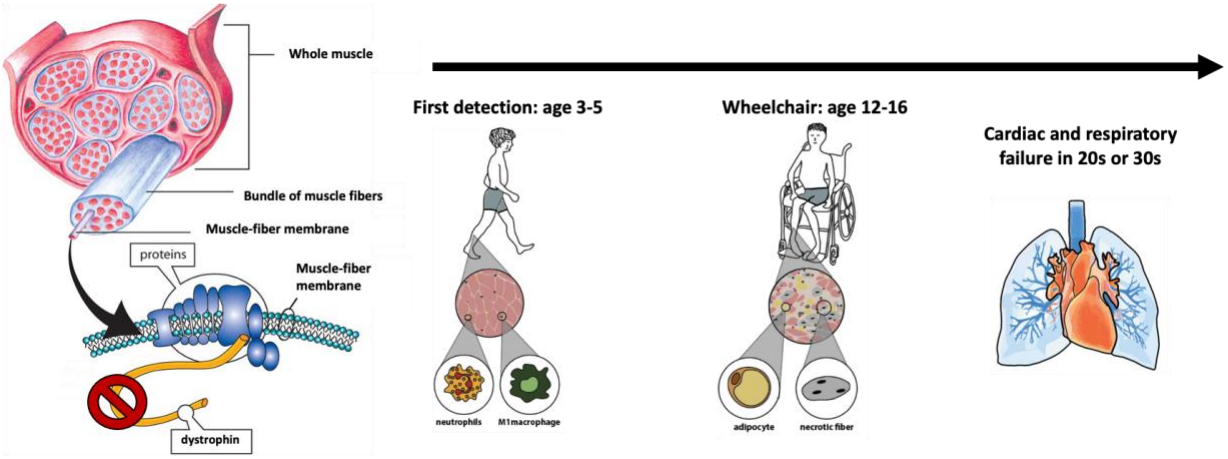

Figure 1.1. Timeline of disease in DMD.

The current standard of care, corticosteroids, will extend the time of ambulation and life by only a few years, and can cause troublesome side effects such as weight gain, decreased bone density, and behavioral issues [6]. Despite recent advancements in gene therapies, and even FDA approval of two exon skipping drug treatments, as of yet, patients see minimal clinical improvement [6]. The lack of effective treatments emphasizes the need for further research and novel tools to better understand and treat DMD.

Computational modeling offers new tools to help reveal complex physiological adaptive processes in dystrophic muscle degeneration that are difficult and expensive to investigate in experiments. Previous computational models have been developed to predict muscle regeneration and disease outcomes, but none offer long-term predictions of skeletal muscle adaptations in DMD *and* take into account stochastic, spatial behaviors of cellular interactions [7,8,9,10,11].

In this thesis, I present a chronic agent-based model of muscle degeneration in the *mdx* mouse. This thesis contains four subsequent chapters. Chapter 2 presents background material on normal skeletal muscle structure and regeneration, how the regeneration process is impaired in DMD, and prior computational models of degeneration and regeneration in skeletal muscle and disease. In Chapter 3, I explain the methods for developing the chronic, agent-based model of DMD, including how the model is changed from previous models and a summary of each of the agents' literature-defined rules. In addition, Chapter 3 explains what damage was inflicted on the muscle to recreate the chronic low, level injuries seen in DMD. Chapter 4 summarizes the results of simulations ran in the model. Chapter 5 discusses the results of the model, and how

the findings add to knowledge of muscle degeneration and DMD. Additionally, limitations of the model and future directions are discussed.

Chapter 2 : Background

2.1 Skeletal muscle structure and regeneration

Skeletal muscle is defined by a hierarchical structure, in which whole muscle is comprised of bundles of fascicles that are made up of contractile muscle fibers [1]. Each muscle fiber is surrounded by a network of extracellular matrix (ECM) that builds the endomysium. The intracellular cytoskeleton of the muscle fiber is linked to that of the ECM through the dystrophin glycoprotein complex (DGC). The smallest force producing unit in muscle is the sarcomere, which is what muscle fibers are comprised.

When injured, skeletal muscle has a robust capacity to regenerate [12]. The regeneration process is complex and dynamic, consisting of many different cell types. Resident macrophages initiate the cascade of regeneration after damage, rapidly recruiting neutrophils that peak within about 24 hours and decline quickly after [13]. Neutrophils condition the inflammatory environment with pro-inflammatory cytokines, including TNF-alpha, MCP, and IFN that activate M1 macrophages. Alongside this early inflammatory response, satellite stem cells (SSCs) are activated and begin to proliferate and differentiate. SSCs are myogenic precursor cells that reside quiescently on muscle fibers, which are activated upon damage and the presence of the growth factors HGF, FGF, and IGF. SSCs divide symmetrically (into 2 SSCs) and asymmetrically (into one

SSC and one myoblast), which allows them to peak within the muscle between three and seven days after an injury [14]. Myoblasts differentiate into myocytes that fuse with the fiber to repair and rebuild the muscle [15]. About 10% of SSCs do not terminally differentiate, and instead will return to quiescence to replenish the reserve SSC pool [14].

Fibroblasts and fibro-adipogenic progenitors (FAPs) are also important in muscle regeneration, as they secrete collagen to rebuild the ECM [13]. The literature often does not distinguish between fibroblasts and FAPs, as they both express PDGFR-alpha. FAPs are triggered by TGF-beta to differentiate into matrix producing cells, as they both express PDGFR-alpha and are considered as the primary producers of connective tissue [16,17]. For simplicity, we will refer just to fibroblasts, although the behaviors encompass behaviors of FAPs as well. Fibroblasts are recruited to damaged tissue based on IL4 that is secreted by eosinophils and M2 macrophages [17]. Studies have also shown important feedback between SSCs and fibroblasts, in which fibroblasts proliferate in the presence of SSCs, and a lack of fibroblasts leads to premature SSC differentiation and impaired regeneration [18]. Population counts reach a peak between three and seven days following an injury, and their apoptosis is caused by TNF-alpha [19]. However, TGF-beta blocks the apoptosis of fibroblasts, and prolonged exposure to TGF-beta will cause differentiation into a myofibroblast phenotype that secretes greater amounts of collagen than regular fibroblasts [19]. A carefully timed switch from a TNF-alpha enriched to a TGF-beta enriched environment has been shown to be crucial in controlling proper matrix deposition. The skeletal muscle regeneration process is implicated in diseases such as Duchenne Muscular Dystrophy, where chronic inflammation, fibrosis, and lead to muscle degeneration [20].

2.2 Duchenne Muscular Dystrophy

Duchenne Muscular Dystrophy (DMD) is a severe muscle wasting disease that affects 1 in every 3,500 boys [5]. Patients with DMD require a wheelchair by age 12, and often die due to respiratory or cardiac failure by the mid 20s. The initiating cause of DMD is known – the absence of dystrophin, a protein that associates with a multimolecular network of integral and

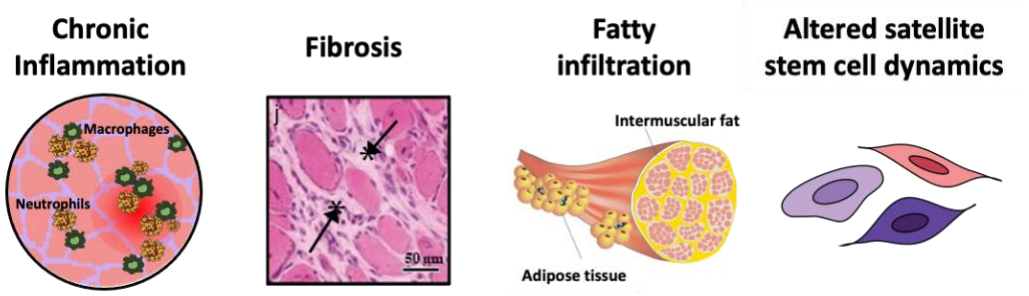

Figure 2.1. Changes in muscle due to DMD.

subsarcolemmal proteins, known as the dystrophin glycoprotein complex (DGC) [2]. Dystrophin and the DGC form a physical link between the intracellular cytoskeleton of the muscle fiber and the extracellular matrix. Without dystrophin, the DGC fails to properly form at the sarcolemma and the link is compromised, which diminishes the strength of the muscle fiber membrane [2]. The weak membrane is susceptible to damage by muscle contractions during everyday movements, which can initiate a cascade of muscle fiber necrosis, chronic inflammation, and ultimately progressing to severe muscle weakness [3,4] (Fig. 2.1). However, despite extensive research and knowing the cause of DMD, there is no cure for DMD, and current treatments have had limited efficacy because promising treatments in mice do not translate to clinical benefit in patients. Treatment is difficult because DMD and muscle regeneration are complex processes, involving mechanisms that transcend spatial and temporal scales.

The lack of dystrophin causes many downstream effects to cell behaviors, growth factor and chemokine levels. The lack of dystrophin alters fibroblast and myofibroblast behaviors, causing increased secretions of collagen, fibronectin, and MMPs in comparison to healthy fibroblasts [21,22]. SSCs have been shown to express dystrophin in wild type mice. However, this expression is lost in DMD, causing a lower proportion of asymmetric cell divisions that are essential in repairing muscle fibers [14]. Additionally, research has shown a rapid decline in number of SSCs starting at 6 months old, suggesting that *mdx* SSCs are unable to maintain a proper balance of proliferation, self-renewal, and differentiation [23]. However, SSCs retain the potential to proliferate, differentiate, and fuse into myotubes at all ages in the *mdx* mouse suggesting that the environment is the reason for SSC decline [24]. This is different in patients with DMD, in which SSC replicative capacity declined with donor age, and this decline was accelerated in DMD in comparison to control SSCs [25].

The *mdx* mouse is the most commonly used animal model to study DMD [26,27]. It is a genetically homologous model of DMD, however, the *mdx* mouse muscle does not degenerate as severely as it does in patients with DMD, with the exception of the diaphragm [28]. In the *mdx* mouse, from 3-4 weeks of age, there is an early episode of widespread skeletal muscle necrosis and significant inflammation [29,30]. By 3 months of age, the mdx mouse has recovered to a more stable phenotype and established a relative resistance to further degeneration. However, at 9 months, the adult mdx mouse is representative of a profibrotic phenotype with impaired muscle regeneration [29]. These changes contribute to the pathological state in the older mdx mouse, which is characterized by severe muscle weakness, loss of muscle weight, and accumulation of fat and fibrosis. To address the milder phenotype found in *mdx* mice, additional

mouse models have been explored, such as the dystrophin-utrophin double knockout mouse [31]. In addition to the lack of dystrophin, the dystrophin-utrophin double knockout mouse lacks utrophin, a transmembrane protein that is found upregulated in *mdx* mice but not DMD patients, leading to a more severe phenotype with increased muscle damage and degeneration.

Translation of pre-clinical trials in mice to patient is greatly hindered by the fact that mouse *mdx* model does not exhibit all of the adaptive processes that are observed in boys with DMD. Despite recent FDA approval of new exon-skipping therapies that aim to reestablish dystrophin in DMD, these treatments have limited success, and corticosteroids, which mitigate inflammation, prevail as the leading DMD treatment [6,32]. However, long-term corticosteroids use causes significant side effects, including weight gain, weak bones, and liver damage [6]. The relative success of corticosteroids highlights the importance of inflammation in dystrophic muscle degeneration. Additionally, studies have shown that due to the progression of inflammation, the time between acute injuries is crucial in determining the muscle response to damage [33]. When a muscle is reinjured while it is within the later proinflammatory regenerating stage, the asynchronously regenerating microenvironments oppose each other, impairing the regeneration process and encouraging development of fibrosis [33]. However, the mechanisms behind how the inflammatory state of the muscle microenvironment affects muscle regeneration are poorly understood, and experiments involving chronic injuries are difficult and costly.

2.3 Prior computational models

Computational modeling provides a powerful to tool to investigate complex behaviors in skeletal muscle that may not be accessible through experiments due to cost or limitations in equipment. Computational models also provide a means to probe individual parameters that

may not be able to be directly probed through experiments. Skeletal muscle models have evolved from simplified Hill-type models representative of cross-bridge mechanics [34,35] into more complex models of human movement using tools such as motion capture, magnetic resonance imaging (MRI), and finite element (FE) modeling that explore muscle dynamics and predict forces, stresses, and strains experienced by muscle [36,37].

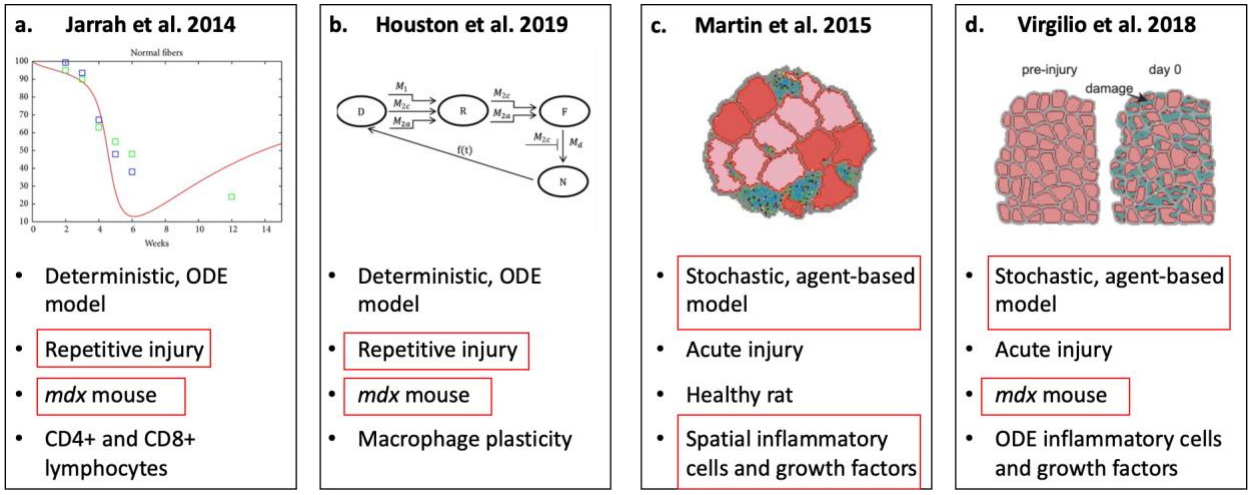

Figure 2.2. Previously published computational models of muscle regeneration in injury and disease. These models range from deterministic, mathematical models (a, b) to stochastic, spatial agent-based models (c, d). The red boxes show aspects of each model that was determined important for a long-term model of disease progression in DMD.

Recently, there have been several models created to predict cellular behavior in muscle degeneration and regeneration, often using agent-based modeling (Fig. 2.2). Agent-based models (ABMs) are particularly useful in studying complex biological processes, such as muscle regeneration, that are dynamic, spatially heterogenous, and stochastic. ABMs represent individual biological cells as computational agents within a tissue will respond emergently to literature-derived rules. Martin et al. developed the first ABM of muscle degeneration due to disuse [38]. Additionally, Martin et al. developed an ABM of skeletal muscle remodeling after an acute injury to explore the role of inflammation in muscle regeneration [8]. He included macrophages, neutrophils, SSCs, and fibroblast agents within the model. Both of Martin et al.'s

models were created using the ABM software, NetLogo. Virgilio et al. developed an ABM that predicts muscle regeneration from injury in DMD, based on interactions between SSCs, fibroblasts, inflammatory cells, muscle fibers, and connective tissue [7]. This model simplified the actions of the inflammatory cells included in Martin et al. by replacing the spatial macrophages and neutrophils with a system of ODEs. Another ABM of skeletal muscle regeneration was created by Westman et al. to elucidate the cellular mechanisms that contribute to failed muscle regeneration in volumetric muscle loss [11]. Both Virgilio et al. and Westman et al. built their models using Repast, a java-based modeling platform (Argonne National Laboratory, Lemont, IL). The contributions of Martin et al., Virgilio et al., and Westman et al., have demonstrated the usefulness of ABMs in simulating complex behaviors in skeletal muscle to predict regeneration.

Other mathematical models have been used to explore muscle regeneration in muscular dystrophy. Dell'Acqua and Castiglione and Jarrah et al. use macrophages, T helper cells, and cytotoxic T cells to predict muscle degeneration and regeneration using a system of ODEs [9,39]. The FRiND model created by Houston et al. presents a mathematical model simulating the effects of macrophage plasticity on dystrophic muscle regeneration [10]. While these models involve less complex modeled interactions between cell types, they offer insight into regeneration from chronic, low level injuries that are experienced in DMD.

The motivation of this thesis is to address the limitations in these prior models, and create a model of dystrophic muscle degeneration that includes spatial interactions of macrophages, neutrophils, SSCs, and fibroblasts in response to chronic, low-level injuries similar to those that are experienced in DMD (Fig 2.4).

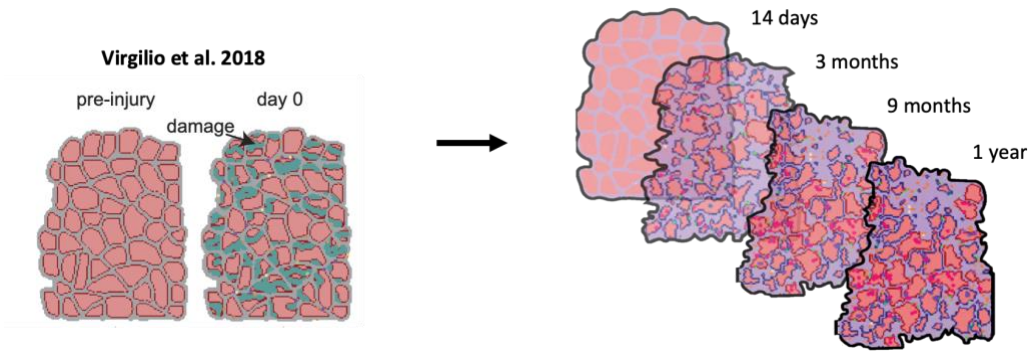

Figure 2.3. The model developed by Virgilio et al. was used as a foundation and adapted to develop a new model that represented repetitive injuries in an *mdx* mouse.

Chapter 3 : Methods: Creating the chronic mdx model

3.1 Goals of Model

The primary objective in developing this model is to predict disease progression in the *mdx* mouse through inflicting daily injuries that are repaired through protein secretion and diverse cellular dynamics. To be successful, the model must capture the increased fibrosis, conflicting inflammatory environment, and decline satellite stem cells (SSC) with age, as corroborated by the literature. Figure 2.1 shows a high-level overview of the framework of the model, including a probability tree for the cell behaviors of fibroblasts, macrophages, neutrophils, SSCs, and their interaction with the microenvironment consisting of muscle fibers, extracellular matrix (ECM), necrosis, and growth factors.

3.2 Agent Based Model Modifications from Previously Published Model

To simulate chronic injuries and disease progression in the *mdx* mouse, a previously published agent-based model of acute injury response in *mdx* skeletal muscle was adapted utilizing Repast Simphony [7]. This model by Virgilio et al. simulated muscle regeneration in the *mdx* mouse through the actions of fibroblasts and satellite stem cells (SSCs) and their interactions with inflammatory cells and growth factors in the microenvironment that were calculated by a series of ordinary differential equations (ODEs). Cell "agents" behaviors included migration, growth factor secretion, division, differentiation, and apoptosis. The environment was made up of a histology-defined muscle cross section, which included muscle fibers and an endomysium made of the extracellular cellular matrix (ECM). A buffer of 5 additional ECM elements was added to each ECM element to allow for migration of agents, and results were normalized by 6 to account for the change. When an acute injury was imposed on the muscle, necrotic elements were added, initiating the simulated regeneration response. While this model served as a base for my chronic injury model, and many of the same defined behaviors remained, several adaptations had to be made to fully recapitulate a full year of the *mdx* mouse. The model was set to start when the mouse is 14 days old, as this is when mice have increased in size, and is slightly before the onset of the disease [40,41].

The biggest change to the model was that the inflammatory agents, specifically neutrophils and macrophages, were redefined as spatial agents. Spatial macrophages and neutrophils had previously been incorporated into an ABM by Martin et al. in NetLogo, but were simplified to create the ABM by Virgilio et al. While the inflammatory spatial cues were

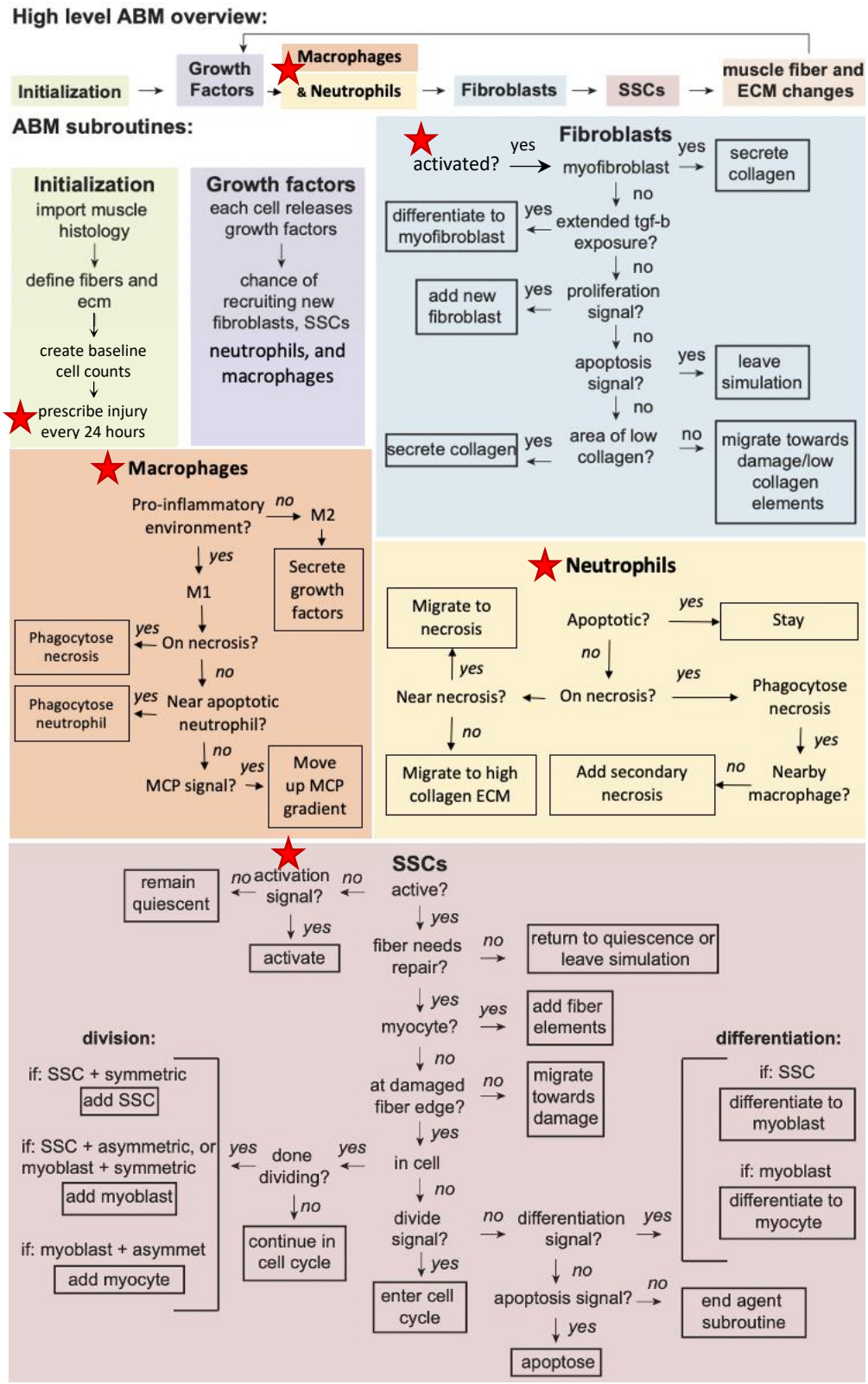

Figure 3.1. Flowchart of ABM rules. First the model is initialized, during each subsequent time step the growth factors are calculated. Then the spatial agents, macrophages, neutrophils, fibroblasts, SSCs, fibers, and ECM follow a probability-based decision tree to guide their actions. In the flow chart, boxes represent a final action for the agent for the current time step. Red stars indicate elements that were added or modified to the model developed by Virgilio et al.

determined to be unimportant in an acute injury, the *mdx* mouse experiences microinjuries that occur before the previous injury has had a chance to fully resolve, creating a conflicting inflammatory environment that leads to chronic inflammation, fibrosis, and impaired regeneration [28]. Therefore, it was important to model the inflammatory cells spatially in order to fully capture the effects of a chronic inflammatory environment.

The environment was defined as pro- or anti-inflammatory based on the growth factor levels, which then led to the recruitment of the corresponding cell-types. With the ODEs used in Virgilio et al., cell recruitment was primarily dependent on the other cell type counts and the initial burst of damage, and therefore was only indirectly influenced by growth factor levels. After inflicting damage, resident macrophages would get recruited and cause the cascade of neutrophils, m1 macrophages, and m2 macrophages to define the inflammatory response in the model. This limited the stochasticity of inflammatory cell type recruitment, which is important in understanding how the conflicting pro- and anti-inflammatory signals in the microenvironment impair regeneration. In changing these inflammatory cell types to spatial agents, their recruitment was directly based on the chemokine and cytokine levels, similar to the inflammatory agents in the ABM by Martin et al. This allowed for a similar cell recruitment cascade, but extended the model to respond to the persistent injuries that disturbed the typical regeneration response.

Additionally, monocyte chemoattractant protein-1 (MCP-1) was changed to be spatial so that it could guide migration of macrophages [42]. This was necessary because the macrophages needed migration cues in the environment to move towards further areas of necrotic tissue after they cleared all necrosis nearby. To transition from ODE calculations to spatial MCP secretion,

Daily microinjuries are inflicted to mimic damage caused by daily use in DMD

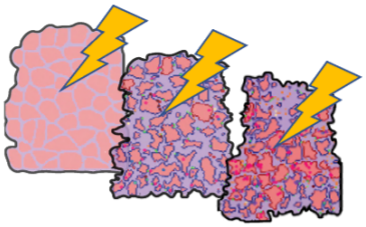

Inflammatory cells are more complex and behave spatially [7]

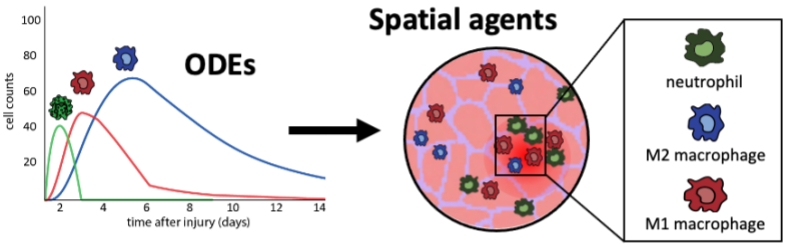

Neutrophils, fibroblasts and SSCs secrete spatial MCP-1 that diffuses to guide macrophage migration [43]

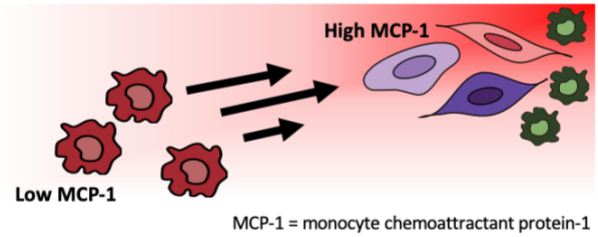

MCP-1 = monocyte chemoattractant protein-1

SSC activation depends on growth factors, rather than recent damage [44,45]

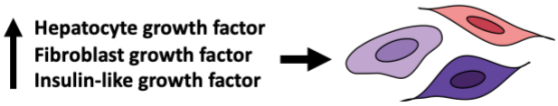

Fibroblast recruitment depends on Il-4 secreted by M2 macrophages and eosinophils [69]

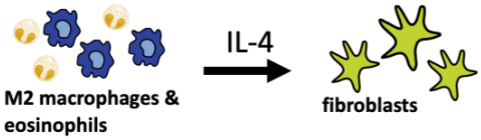

Figure 3.2. Summary of modifications to the ABM developed by Virgilio et al. to develop a new, long-term model of disease progression in DMD.

the agents would secrete MCP every hour at their location, and the MCP would diffuse into the neighboring ECM and fibers, and decay at the same rate as it was defined to in the ODEs. MCP was secreted by neutrophils, and when the environment was inflammatory, by SSCs and fibroblasts [42,43]. The environment was considered inflammatory when there was a greater amount of TNFa than TGFb in the environment [19]. The secreted spatial MCP was confirmed to match the ODE values of MCP at each time point. Therefore, for any case within the model that utilized MCP level, the total amount of spatial MCP was calculated and used instead without disrupting other model calculations. The spatial MCP was recognized by macrophage agents, which would migrate up the MCP gradient. This allowed M1 macrophages to move towards areas of damage and clear the necrotic tissue.

Further changes were also made to the rules that govern the recruitment of fibroblasts and SSCs to make these behaviors more dependent on growth factor secretions. SSC activation was induced by HGF, FGF, and IGF, based on data from the literature [44,45]. In Virgilio et al., SSC activation was solely dependent on the damage signal after injury. This change showed a lower peak of SSCs than previously, however the muscle fiber CSA recovery was comparable to the model, and therefore these changes were considered acceptable. Future iterations could explore increased satellite cell activation to refine the data. Additionally, fibroblast recruitment was altered due to changes in the secretion of IL4. Fibroblast recruitment is directed by IL4 levels in the environment, and previously in Virgilio et al., IL4 was only secreted based on the eosinophils that are calculated based on initial burst of damage, which was limiting for the daily microinjuries. To mitigate this, M2 macrophages were set to secrete IL4 in addition to the eosinophils [69].

Validation of healthy and *mdx* muscle was done by comparisons to muscle fiber CSA recovery and cell counts from Virgilio et al. In healthy muscle, the chronic ABM was set to the original, healthy growth factor secretions and asymmetric division (Table 3.2), and a 10% acute injury was prescribed at the start. In dystrophic muscle, the chronic ABM was set to dystrophic growth factor secretions and decreased asymmetric division (Table 3.2), and a 35% acute injury was inflicted at the start.

3.3 Agent Based Model Rules Summary

Macrophages and Neutrophils

At initialization, resident macrophages are placed randomly and homogenously throughout the ECM. Following an injury, resident macrophages secrete inflammatory factors to recruit neutrophils. Neutrophils are placed in areas of necrosis, where they then phagocytose necrotic tissue [46]. When phagocytosing necrotic tissue, secondary damage is caused to nearby muscle fibers, although the fiber is protected if there is a neighboring macrophage [46]. After phagocytosis, neutrophils have a chance of apoptosing [46]. The neutrophils remain in the environment for only 1-2 days after recruitment [13]. Macrophages are recruited by growth factors and cytokines in the environment, as detailed in Table 3.1. Macrophage recruitment is further compartmentalized into pro-inflammatory M1 macrophages and anti-inflammatory M2 macrophages, each of which is weighted based on the growth factors and cytokines present in the environment [8]. If an M1 macrophage is on an area of necrosis, it will phagocytose that necrosis and replace it with an ECM element of low collagen. If an apoptotic neutrophil is within the vicinity of the M1 macrophage, that apoptotic neutrophil will be phagocytosed. After phagocytosis of an apoptotic neutrophil, the macrophage has a chance of transitioning into an

M2 macrophage [49]. If the M1 macrophage is not near necrosis or an apoptotic neutrophil, it will migrate up the MCP gradient [42]. If there is no MCP detected nearby, the macrophage will choose a random neighboring ECM element to migrate to. M2 macrophages secrete important anti-inflammatory growth factors and chemokines including TGF-beta, IL-10, and IL-4 that promotes the recruitment of fibroblasts and deters recruitment of pro-inflammatory cell types [13]. Specific rules on macrophage and neutrophil behavior are found in Table 3.1.

SSCs (myoblasts, myocytes)

At the initial time point of the simulation, one quiescent SSC agent per four fibers was placed on the fiber edge. After injury, SSCs were activated by HGF, FGF, and IGF and recruited to injured muscle fibers [44,45]. To drive muscle fiber repair, SSCs will divide asymmetrically by adding a new myoblast. SSCs also divide symmetrically, by adding another SSC, to grow and maintain the SSC pool [14]. After differentiation into myoblasts and further differentiation into myocytes, the myocytes add fiber elements along the injured fiber border. After the muscle fiber that the SSC is associated with is fully repaired, SSCs return to quiescence. If there are more SSCs than M1 macrophages, the SSCs have a chance of apoptosing that is scaled by the total number of M1 macrophages [43]. Specific rules on SSC activation, division, secretion, and quiescence are found in Table 3.1.

Fibroblasts (myofibroblasts)

When the model is initialized, fibroblasts are distributed homogeneously throughout the ECM and additional fibroblasts are recruited by IL4 following an injury [13,47].

Proliferation of fibroblasts occurred when there were activated SSCs in the environment. After extended exposure of 12 hours to TGF-beta, fibroblasts differentiate into myofibroblasts [8]. Fibroblasts and myofibroblasts secreted collagen and fibronectin to rebuild the ECM, as well as other growth factors detailed in Table 3.1. Apoptosis is caused by the presence of TNF-alpha, and is blocked if there is more TGF-beta than TNF-alpha in the environment [19]. Specific rules on fibroblast behavior are found in Table 3.1.

ECM and Necrosis

The grid which the cell type agents moved on was made up of muscle fiber, ECM, and necrosis elements. When an injury was prescribed to the model, necrotic elements replaced muscle fiber. When necrosis was cleared by either neutrophils or M1 macrophages, the corresponding elements were replaced by low-collagen ECM. Fibroblasts secreted collagen in these low-collagen areas, to rebuild the muscle and restore stiffness to the damaged tissue [16-19]. If areas of low collagen persisted, neighboring ECM elements merged to form a single collagen element made up of the combined collagen amount. To grow muscle fibers, myocytes fuse to the fiber edge to add new fiber elements [15,49].

Table 3.1. Summary of Agent Behaviors

Agent	Subtype	Rules	References
Macrophage	**General**	Recruited by CCL4, CCL17, CCL13, IL6, and MCP	[8],[13]
		Deterred by PGE2, lipoxins, TGFβ	[8],[13]
		Either M1 or M2, weighted by environment (see M1 and M2 in table)	[8]
		20% chance of death after 40 hours	[13],[48]
	Resident	Proliferates if there is new damage	[13]
		Returns to baseline levels when there are neutrophils present or if they are > 5 hours old	[7],[8]
		Secretes:	
		TNFα, IL1, IL8, CXCL2, CXCL1, CCL3, CCL4	[13],[54]
	M1	Chance determined by IFN and TNFα	[13],[46],[54]
		Migrates toward nearby necrosis, apoptotic neutrophils, or up the MCP gradient	[42]
		Phagocytoses necrotic tissue and apoptic neutrophils	[48],[49]
		Chance of transition to M2 phenotype after phagocytosis of neutrophil, increases when age > 35 hours	[48],[49]
		Secretions:	
		Non-phagocytosed: TNFα, IGF, IL1, IL8, IL6, IFN, MMP12, GCSF, IL10,	[48],[49]
		Phagocytosed Necrotic Tissue: TNFα, IGF, IL1, IL8, IL6, IFN, VEGF, MMP12, GCSF, lipoxins, resolvins	[48],[49]
		Phagocytosed Apoptotic Neutrophil: TGFβ, TNFα, IGF, IL1, VEGF, MMP12, GCSF, IL10, lipoxins, resolvins	[48],[49]
	M2	Chance determined by IL10 and IL4	[13],[48],[49],[54]
		Secretions:	
		TGFβ, TNFα, IGF, IL10, CCL17, CCL22, collagen4, PGE2, IL4	[13],[48],[49]
Neutrophils		Recruited by IL1, GCSF, MCP, CCL4, CXCL1, IL8, and necrosis	[8],[13],[46]
		Deterred by lipoxins, resolvins, MMP12, lactoferins, PGE2, IL10, and IL6	[8],[13],[46]
		At each time step, if the recruitment force is higher than dettering force, add up to 12 neutrophils	[8],[13]
		If there is recent damage and resident macrophages, there Is a chance to override determent	[46]
		Neutrophils get added to new areas of necrosis	[46]
		Migration toward necrosis or ECM	[8],[13]
		Phagocytosis of necrotic tissue	[46]
		Secrete MCP at location	[46]
		If nearby a fiber and not any macrophages, change fiber element to secondary necrosis	[46]
		Secretions:	
		TNFα, IL1, IL8, CCL3, IL6, MCP, IFN	[8],[13]
		Apoptotic: VEGF, lactoferins, HGF	[8],[13]
		Chance of death	
		After phagocytosis, 25% chance of death	[8],[46]
		After 8 hours, 20% chance of death	[8],[46]
SSCs		Activation	
		Induced by HGF, FGF, and IGF	[44],[45]
		Division	
		Induced by IGF, FGF, TNFα, IL6, VEGF, PDGF, GCSF	[7], [43]
		Prevented by IL10 and IL4	[7],[42],[44],[48]
		Assymmetric or Symmetric chance based on healthy or disease	[7],[14],[42],[44],[48]
		Secretions:	
		MMPs, fibronectin, IL1, IL6, MCP, CCL22	[15],[42],[43]
		Inflammatory dependent: TNFα, MCP-1 and IL8	[43]
		Quiescence	
		If associated fiber CSA is recovered	[13],[14]
		Apoptosis	
		If there are more myoblasts than M1 macrophages, chance is scaled by total number of M1 macrophages	[43]
Fibroblasts	**Active**	Recruited by IL4 secreted by eosinophils and M2 macrophages	[13],[17],[47],[69]
		Proliferation based on SSC counts	[18]
		Extended TGFβ exposure causes transition into myofibroblast	[19]
		Secretions:	
		Collagen to rebuild ECM	[13],[16],[17],[21]
		latent TGFβ, IGF, PDGF, MMPs, fibronectin, IL6, FGF	[13],[22]
		Inflammatory dependent: IL1, IL8, MCP	[71]
		Migrates towards areas of low collagen	[71],[72]
		Apoptosis by TNFα, blocked by TGFβ - if both growth factors are similar, there is a 50% chance of apoptosis	[19]
	Myofibroblast	Secretions:	
		2x as much collagen as fibroblasts	[21]
		Active TGFβ, MMPs, fibronectin	[21],[22]

3.4 Simulating a healthy vs. mdx mouse

The lack of dystrophin causes many downstream effects to cell behaviors, growth factor, and chemokine levels. Several changes were made to distinguish how injury progresses in a dystrophic vs. healthy environment. Growth factor calculations were modified based on literature data to recapitulate the changes seen in dystrophic muscle. For example, TNF-a concentration was found to be elevated in *mdx* mice at the onset of damage [50]. To mimic this change, secretion of TNF-a by resident macrophages, neutrophils, M1 macrophages, and inflammatory SSCs was doubled under dystrophic conditions. This allowed for a stronger inflammatory response at the onset of the damage when there are higher numbers of macrophages and neutrophils, followed by a transition to an anti-inflammatory, TGF-beta rich environment within 3-6 months as the M2 macrophages and fibroblasts became more dominant. Higher TGF-beta secretion by fibroblasts and myofibroblasts was explored with the model, but ultimately secretion was kept the same. Zanotti et al. reported unchanged TGF-beta transcript levels in DMD fibroblasts, but increased TGF-beta protein levels when fibroblasts are cultured in DMD medium [21]. To decide whether to alter TGF-beta secretions by fibroblasts, the model was tested with both higher and normal TGF-beta secretion by fibroblasts. Simulations with increased TGF-beta secretion led to almost full depletion of normal fibers, while normal TGF-beta secretion allowed for recovery that better matched literature data. Therefore, the amount of TGF-beta secretion was not changed for dystrophic simulations in the model, and any emergent changes in TGF-beta levels were instead triggered by increased fibroblast and M2 macrophage levels or changes in the environment. Although TGF-beta secretions were not altered in the model, fibroblast and myofibroblast collagen secretion were increased 5 and 1.5-fold, respectively, to

match data published in the literature [21]. Fibronectin secretion was also increased 5-fold to match data published in the literature [22]. Additionally, Zannoti et al. reported a decrease in MMP secretion in dystrophic fibroblasts, but an increase in MMP secretion in myofibroblasts, so MMP secretion was changed accordingly. SSC function is also affected by the lack of dystrophin [21]. Loss of dystrophin expression causes decreased asymmetric division, which cause fewer myoblasts to form. Based on results from Dumont et al., dystrophic SSCs were simulated to divide asymmetrically in only 10% of divisions, in comparison to 50% asymmetric divisions that occurs in wild type mice [14].

Table 3.2. *Changes made to the model to represent a dystrophic phenotype*

Agent Behavior	Healthy	*Mdx*	References
Chance of Asymmetric Division	0.5	0.1	Dumont et al.
Fibroblast secretion of collagen	0.43	2.15	Zanotti et al.
Fibroblast secretion of MMPs	1	0.18	Zanotti et al.
Fibroblast secretion of fibronectin	2	10	Mezzano et al
Myofibroblast secretion of collagen	1.5	2.25	Zanotti et al.
Myofibroblast secretion of MMPs	1	5.23	Zanotti et al.
TNF-alpha secretion	1	2	Munoz-Canoves and Serrano

3.5 Damage Protocols

In order to determine the *mdx* response to multiple injuries, several different damage protocols were implemented. The absence of dystrophin causes reduced strength in the muscle membrane, rendering the muscle susceptible to damage by muscle contractions during everyday movements [2]. In this ABM daily microinjuries were inflicted to simulate the response chronic injury response. Damage to healthy and dystrophic mouse muscle was applied daily at

the following levels: 0.25%, 0.5%, and 1% of total fiber area was replaced with necrosis. Additional simulations were run to inflict damage every 3 days instead of every day.

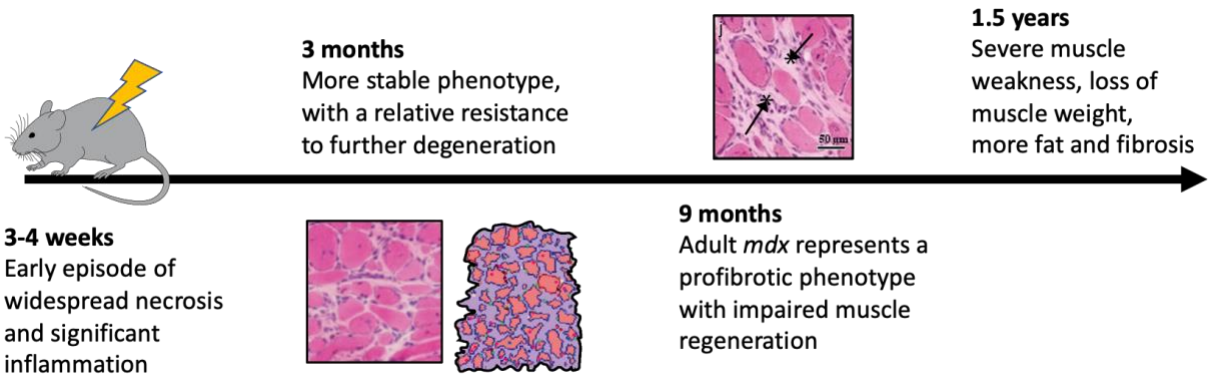

Figure 3.3. Timeline of mdx mouse lifespan. From 3-4 weeks of age, there is an early episode of widespread skeletal muscle necrosis and significant inflammation. By 3 months of age, the mdx mouse has recovered to a more stable phenotype and at 9 months, the adult mdx mouse is representative of a profibrotic phenotype with impaired muscle regeneration.

To mimic how damage changes during disease progression in the mdx mouse, we simulated decreasing levels of damage over time. From 3-4 weeks of age, there is an early episode of widespread skeletal muscle necrosis and significant inflammation (Fig 3.2) [29,30]. By 3 months of age, the mdx mouse has recovered to a more stable phenotype and established a relative resistance to further degeneration. However, at 9 months, the adult mdx mouse is representative of a profibrotic phenotype with impaired muscle regeneration. These changes contribute to the pathological state in the older mdx mouse, which is characterized by severe muscle weakness, loss of muscle weight, and accumulation of fat and fibrosis. Therefore, to simulate how damage changes over time in the mdx mouse, damage was set to 2% for the first 2 weeks, 1% until 3 months old, 0.5% until 6 months old, and finally 0.25 % for the remaining time. Additional simulations were also run where 0.5% damage was maintained after 6 months old, instead of the decay to 0.25% damage. Simulations were run for 1 year. Fibrosis was calculated as fold change in ECM percentage of total.

Chapter 4 Chapter 4: Results – Does the model capture *mdx* mouse disease progression?

4.1 Comparison against previously published acute injury model

The predicted responses to injury in the healthy and mdx mice were validated by comparing muscle fiber CSA recovery and inflammatory cell, fibroblast, and SSC counts to those published in Virgilio et al. The healthy muscle was predicted to experience a decreased fiber CSA for the first 5 days in comparison to Virgilio et al., however by 28 days, the muscle had fully recovered to a fiber CSA that was not significantly different to Virgilio et al. (Fig. 4.1). The CSA recovery throughout the 28 days stayed within the range of experimental regeneration data for healthy muscle following injury [70].

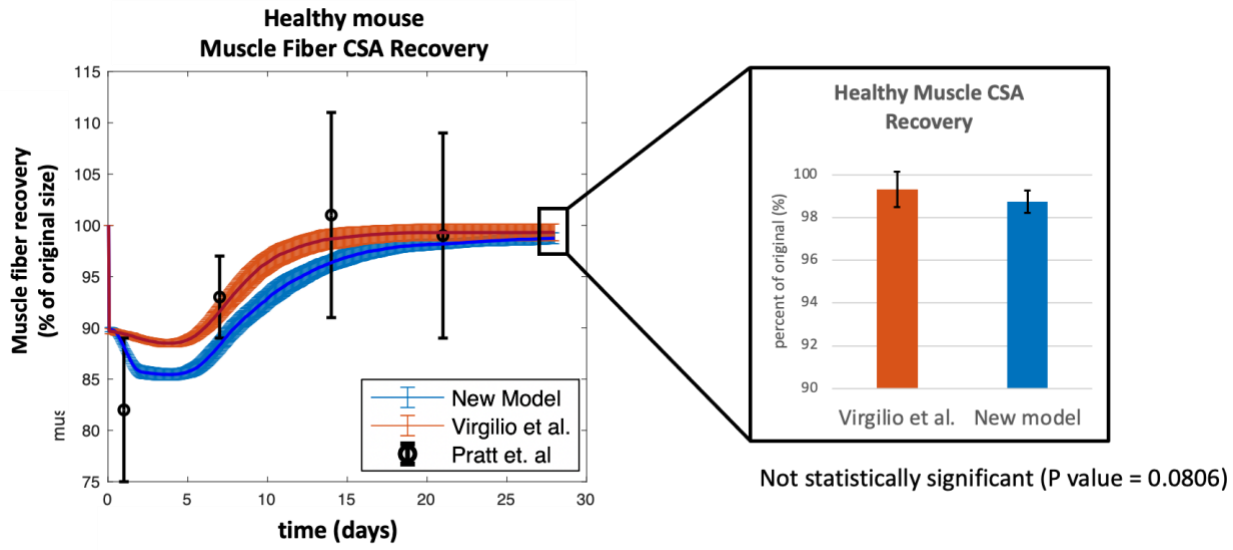

Figure 4.1 Validation of healthy acute injury. Healthy muscle recovery predictions after an acute injury of 10% of muscle fibers in the new model was compared to the model developed by Virgilio et al. and to published experiment results of torque recovery from Pratt et al.

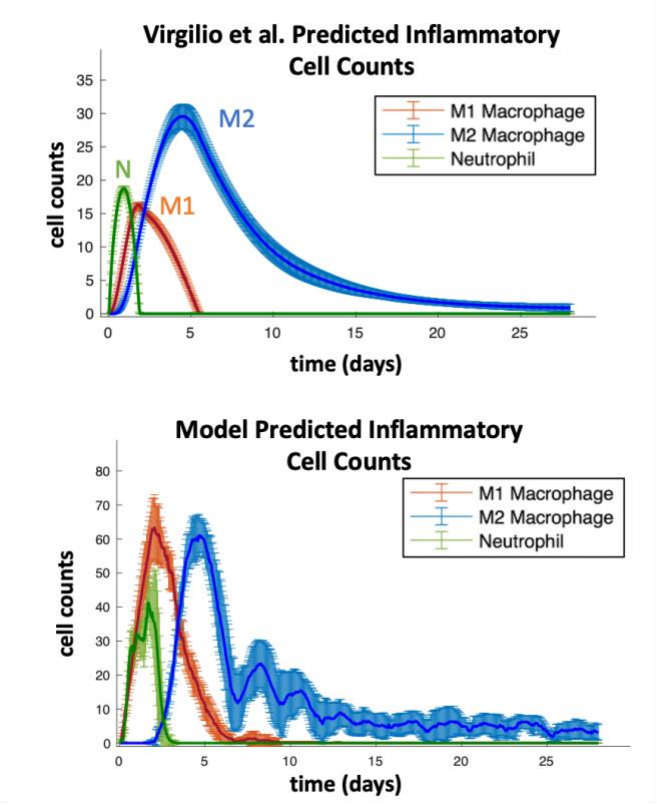

Figure 4.2. Inflammatory cell prediction comparison. Macrophages and neutrophils were compared between predictions from the new model vs predictions from Virgilio et al.

All of the inflammatory cells follow the same time course as in Virgilo et al., starting with the recruitment of resident macrophages, followed by neutrophils that are recruited but leave the muscle within 2 days (Fig. 4.2). M1 macrophages are slower to be recruited and peak at 2-3 days, but remain in the tissue until 5 days post-injury. M2 macrophages in this model and in the model by Virgilio et al. begin getting recruited within 1-2 days after injury, and peak on day 5. The M2 macrophages decline at rates that are similar to Virgilio et al.; however, the decline is not as gradual due to the stochasticity of the agent M2 macrophage behavior. The macrophages and neutrophils are consistently elevated in this model compared to cell counts in Virgilio et al. This is likely because in the transition from ODE to spatial inflammatory agents, cell counts had to be tuned to ensure that necrosis was fully cleared within 2 days to match Virgilio et al. In this model, macrophages and neutrophils had to be proximal to necrosis in order to phagocytose any necrotic tissue, which was distinct from Virgilio et al. in which the shear presence (and not spatial proximity) of macrophages allowed for clearing of necrosis.

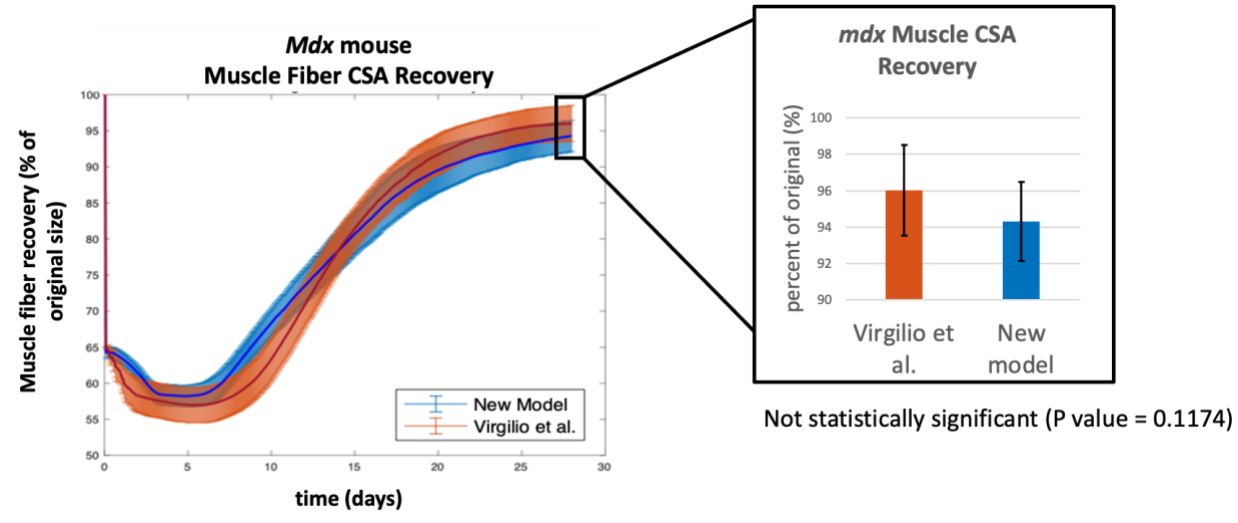

Figure 4.3 Validation of *mdx* acute injury. Healthy muscle recovery predictions after an acute injury of 35% of muscle fibers in the new model was compared to the model developed by Virgilio et al.

Dystrophic muscle fiber CSA recovery following injury closely matched that predicted by Virgilio et al. (Fig 4.3). This model begins regenerating at an earlier timepoint than Virgilio et al.; day 7 and day 8, respectively, but the rate of recovery by Virgilio et al. is faster and ultimately ends with a higher final fiber recovery. M1 macrophage counts match between the new model and Virgilio et al., however M2 macrophages peak at a significantly lower value compared to Virgilio et al., 65 vs 105, respectively (Fig. 4.4a,b). SSC counts are also significantly lower in the new model in comparison to Virgilio et al., with peak counts at 70 and 125, respectively (Fig. 4.4c,d). Fibroblasts follow a very different trend than Virgilio et al., in which counts remain steady following recruitment (Fig. 4.4c,d). In the new model, fibroblasts increase similarly to Virgilio et al. the first day, but then rapidly decline, likely due to the increased TNF-alpha secretion by M1 macrophages. This spike does not occur in fibroblast predictions of the healthy mouse, which supports that it is the increased TNF-alpha causing the change. After this decline, the fibroblasts rapidly proliferate, corresponding to the peak of M2 macrophages, which secrete IL4, a cytokine that recruits fibroblasts. After 25 days, the fibroblasts decline to approximately 50, similar to the

fibroblast count predicted by Virgilio et al. (Fig. 4.4c,d). While there are several differences between the new model and Virgilio et al., the new model captures muscle fiber CSA recovery and M1 macrophage levels well and produces a similar time course of M2 macrophages and SSCs and therefore was considered a good model for injury response in dystrophic muscle.

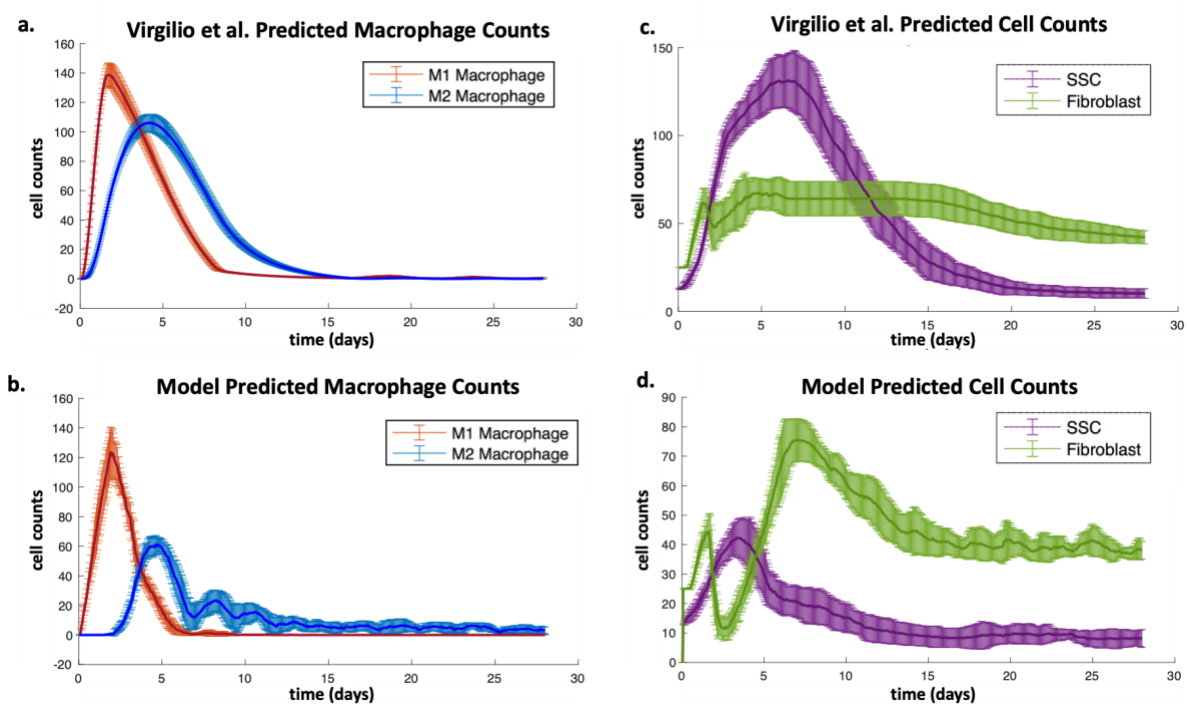

Figure 4.4 Comparison of predicted cell counts in mdx acute injury. Predicted macrophage counts (a, b), SSC and fibroblast counts (c, d), after a 35% acute injury in the new model compared to Virgilio et al model predictions.

4.2 Comparison with previously published experiments of long-term muscle remodeling in mdx muscle

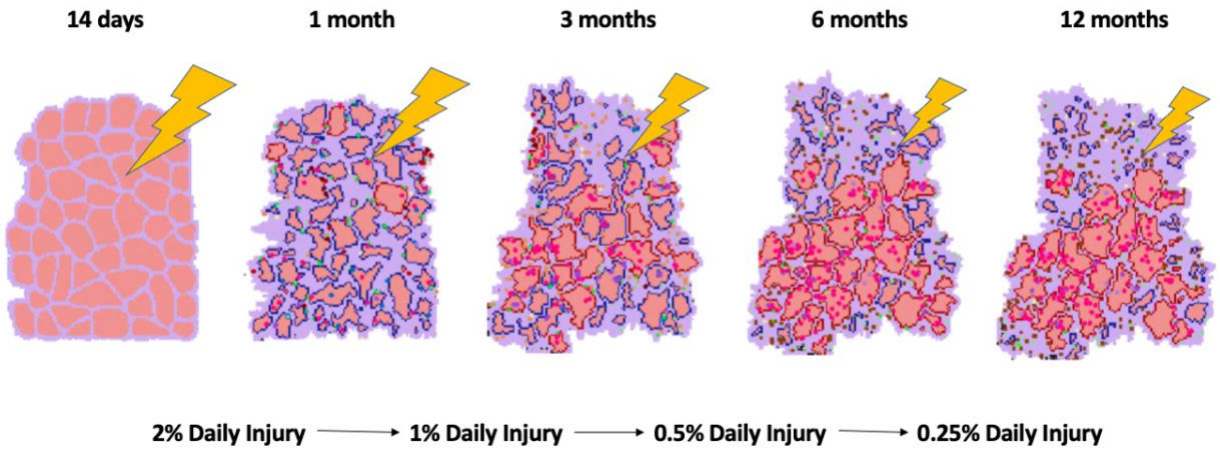

Figure 4.5. Variable Damage was simulated in the mdx mouse model.

As the previously discussed results demonstrated that constant damage inflicted upon skeletal muscle in the model is not sustainable, therefore, simulations that decrease the damage inflicted over time were tested (Fig 4.5). Prior models of chronic injury in the mdx mouse have also found that degeneration is best captured by using a model of decaying damage over time [9,10]. The mdx mouse sees an onset of damage after 14 days old, with damage peaking at 1 month [41], which is represented in the model as 2% damage inflicted daily for the first 2 weeks, followed by a decreased 1% damage. After this widespread initial damage, the mouse recovers to a more stable phenotype at 3 months, with some fibrosis present, and accordingly, damage was decreased to only 0.5% per day. After 6 months, the mdx mouse experiences increased fibrosis and impaired muscle regeneration, so the damage was further reduced to only 0.25% daily. All of these changes are captured within literature data quantifying changes in fibrosis, SSC counts, and muscle volume that was used as validation for the model [23,41,51-59]. Literature

data varied greatly because many different studies were used in order to capture a full year of disease progression, and within these studies several different muscles were observed, including the diaphragm, soleus, quadriceps, EDL, and tibialis anterior. It has been shown that different muscles experience significantly different disease progressions, with the lower limbs experiencing less fibrosis and degeneration in comparison the diaphragm of the mdx, which is more severe and most similar to DMD patients [28].

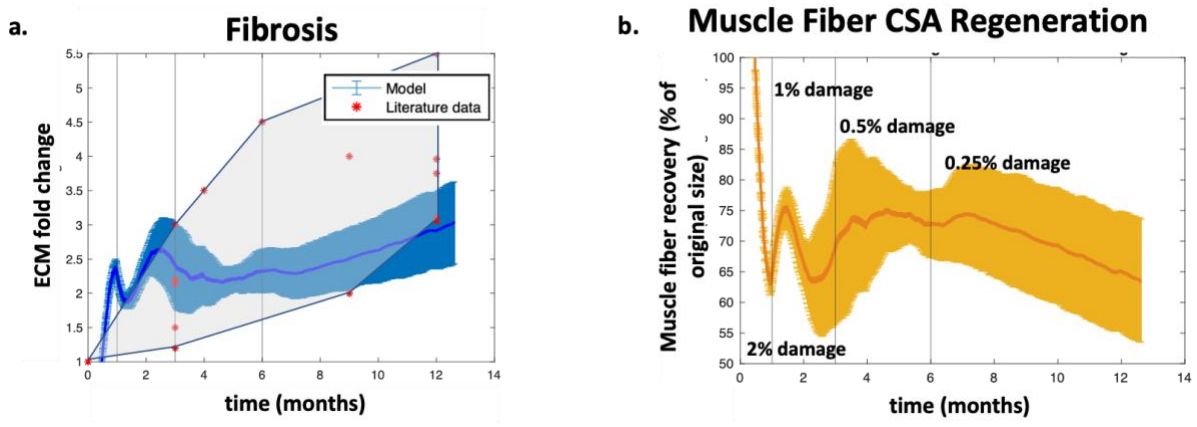

Figure 4.6. Fibrosis and CSA predictions from variable damage schedule in an mdx mouse. Fibrosis (a) and muscle fiber CSA recovery (b) after a variable damage schedule of 2% for the first 2 weeks, 1% until 3 months, 0.5% from 3-6 months, and 0.25% after 6 months. Normalized literature data is represented as red stars and the range of literature is shown by the grey region.

With the variable damage protocol, the model captures the peak onset of damage that levels off after 3 months leaving some increased fibrotic tissue, followed by a relatively stable period up until 8 months when fibrosis begins to increase at a much faster rate (Fig. 4.6). SSC counts throughout the model follow a similar trend to literature data, peaking at around 3-4 months and declining steadily with age (Fig. 4.7a). However, SSC counts in the model peak at a much lower value than in the literature, ~75 rather than 200, respectively. The SSC counts were also lower in comparison to the ABM by Virgilio et al., suggesting that there are important variables or interactions that the chronic ABM is lacking. Despite the low SSC counts, fiber

regeneration after acute injury was not impaired significantly in comparison to Virgilio et al., so it does not necessarily invalidate the model.

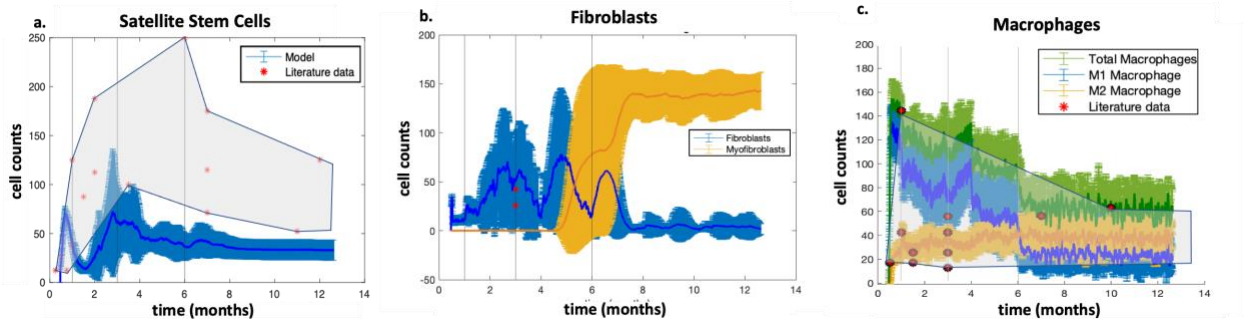

Figure 4.7 Cell count predictions from variable damage schedule in an *mdx* mouse. SSC (a), fibroblast (b), and macrophage (c) cell counts after a variable damage schedule of 2% for the first 2 weeks, 1% until 3 months, 0.5% from 3-6 months, and 0.25% after 6 months. Normalized literature data is represented as red stars and the range of literature is shown by the grey region.

Fibroblasts and macrophages also exhibit interesting behaviors, particularly around 6 months, which is also the time that SSC counts level off and the muscle fiber CSA declines (Fig. 4.7b,c). As all these factors are interdependent in some way, it is difficult to determine which change in agent or environment first caused the decline in regeneration and conveys the complexity of the muscle regeneration process. Starting at approximately 5 months, fibroblast begin to be replaced by myofibroblasts which reach a steady state at around 8 months and do not decline further (Fig. 4.7b). Starting at 4 months, there is a steep decline in M1 macrophages and at 6 months of age, the M2 macrophages become the predominant phenotype (Fig 4.7c). 6 months also corresponds to the decreased damage inflicted. This decline in M1 macrophages likely causes the transition to myofibroblasts, as these M1 macrophages are secreting growth factors and cytokines, such as TNF-alpha, that create a pro-inflammatory environment and encourage fibroblast apoptosis, while M2 macrophages secrete anti-inflammatory growth

factors such as TGF-beta and IL-4 that recruit fibroblasts, encourage the transition into myofibroblasts, and block fibroblast apoptosis.

4.3 Sensitivity of long-term muscle remodeling to varying levels of constant damage

Daily infliction of a constant level of damage to both healthy and dystrophic muscle caused muscle fiber degeneration and increased fibrosis. Lower levels of daily damage (0.25% and 0.5%) allowed both dystrophic and healthy muscle to maintain their fiber size and ECM until around 6-8 months (Figs. 4.8 & 4.9). At this time, fiber CSA begins a rapid decline, while the amount of fibrosis increases to make up for the loss of muscle fibers, except for the 0.25% damage on the mdx mouse, which experiences a slow decline that starts to steepen at 11 months. While relatively similar in response to the lower levels of damage, the dystrophic and healthy mice differ significantly in fiber atrophy when daily damage is increased to 1% (Fig. 4.8). The healthy mouse experiences hypertrophy within the first 2 months, recovering similarly to lower levels of damage, increasing muscle fiber CSA by 9%, while the mdx mouse never fully recovers CSA, peaking at 89% of the original CSA at around 1 month old. Both the mdx and healthy mouse simulations only experience recovery until 1-2 months, and then begin a steep decline for the rest of the duration. This is much earlier than the lower levels of damage, which start their muscle fiber CSA decline after around 6 months. Unexpectedly, the simulated mdx mouse does not degenerate as rapidly as the healthy mouse for each damage amount. This is particularly notable in the 1% daily damage simulation, because the healthy mouse regenerates and even hypertrophies in the first 3 months, but because the mdx is a slower, steadier decline, by the end of one year the *mdx* mouse is twice the size of the healthy mouse muscle fibers. Another

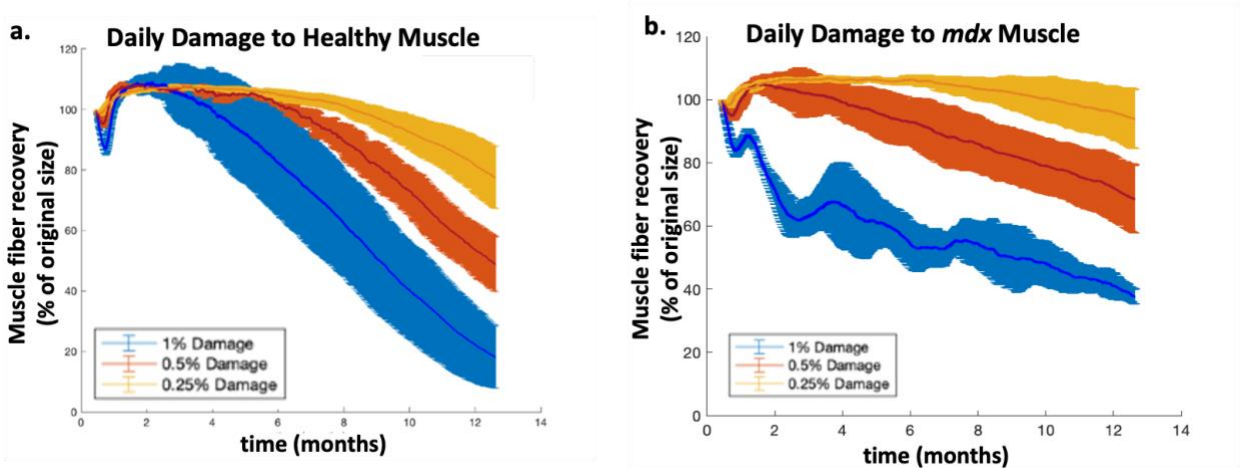

Figure 4.8. Muscle fiber CSA recovery in healthy and mdx mice. A comparison of muscle fiber recovery in healthy (a) and *mdx* (b) mice at 0.25%, 0.5%, and 1% daily damage for 1 year.

interesting finding from the various constant daily damage protocols was that when 1% damage was inflicted on the *mdx* mouse, fiber CSA did not constantly decline constantly as found in the other simulations, but instead experienced fiber growth several times throughout the duration.

An increase in fibrosis after one year Is seen in each damage simulation for both healthy and mdx mice. Fibrosis starts to increase at around 6 months for low levels of damage in healthy mice (Fig 4.9). Fibrosis starts to increase from the onset of damage for each 0.25%, 0.5%, and 1% daily protocols in *mdx* mice and continues to gradually increase the entire duration. At low levels of damage, the end fibrosis between healthy and *mdx* mice is similar, but at 1% daily damage, the healthy mouse experiences significantly increased fibrosis than the mdx after a year, a 9-fold increase vs only a 5-fold increase. It is unexpected that the mdx mouse experienced less fibrosis than the healthy mouse. However, it should be noted that the fiber size is also much smaller in the healthy mouse after 1 year of daily 1% damage, and as fibrosis is considered as the increase in percentage of the ECM in comparison to the total area, the same amount of ECM would contribute to higher fibrosis if the muscle fibers were smaller.

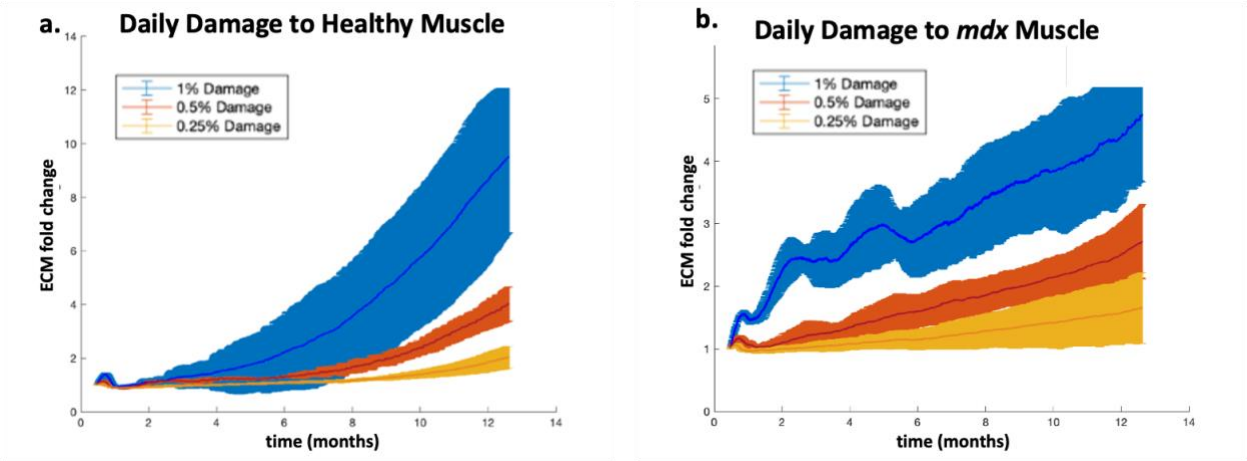

Figure 4.9. ECM fold change in health and mdx mice. A comparison of ECM fold change in healthy (a) and mdx (b) mice at 0.25%, 0.5%, and 1% daily damage for 1 year. ECM fold change is calculated as the change in total percentage of ECM compared to baseline ECM percentage.

Another damage simulation was tested in which the muscle was damaged 1% every 3 days in the *mdx* mouse model (Fig. 4.10). This provided the muscle fibers more time to regenerate following an injury prior to getting injured again. The fiber CSA remains somewhat constant for the first 3 months, and then starts to decline steadily until reaching 73% of the original CSA after 12 months. The fold change in ECM changes linearly over time reaching almost 3x the initial amount. M1 and M2 macrophages maintain constant fluctuations with each new injury, but M1 and M2 counts are relatively the same the entire time. SSCs remain very low throughout the entire 12-month duration, never reaching above 50.

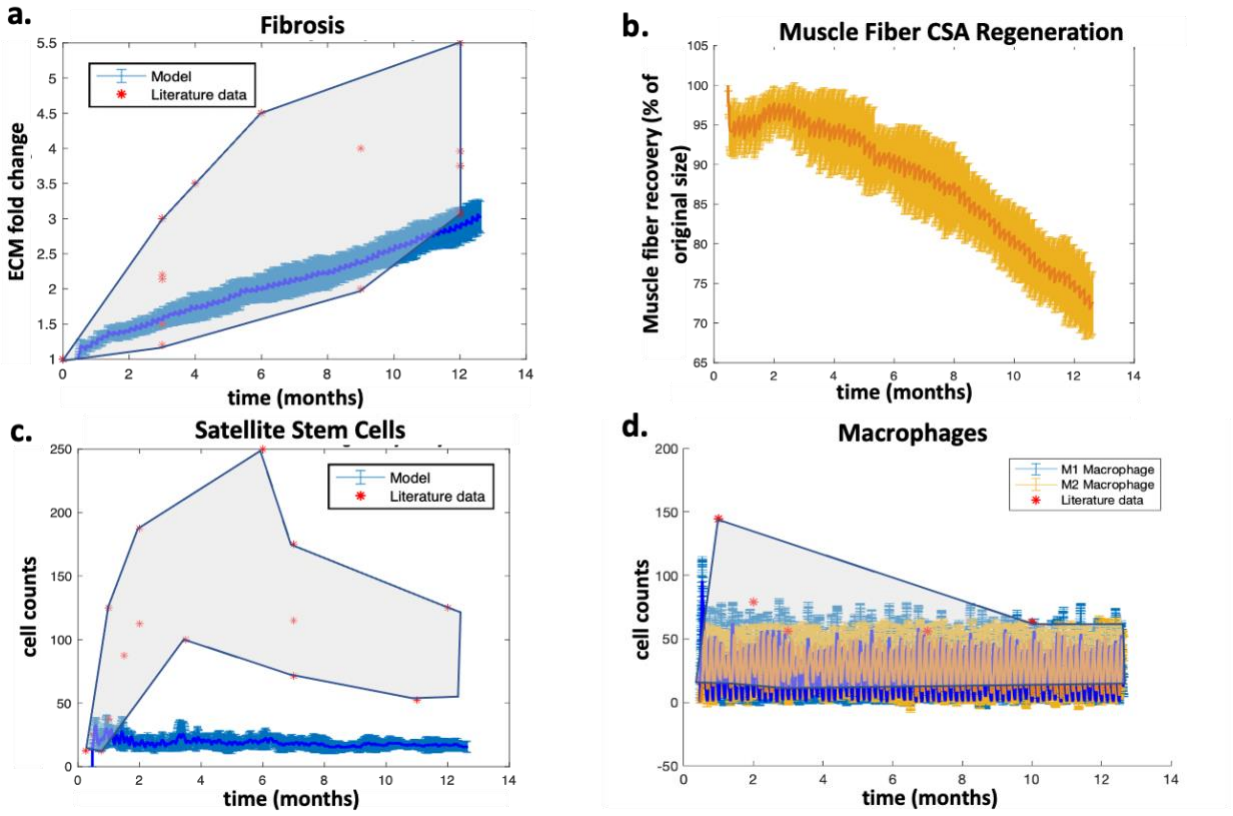

Figure 4.10. 1% damage every 3 days. Fibrosis (a), muscle fiber CSA recovery (b), SSCs (c), and macrophage counts (d) after 1% damage inflicted every 3 days to an mdx mouse for 1 year. Normalized literature data is represented as red stars and the range of literature is shown by the grey region.

Chapter 5 : Discussion, Limitations, and Future Directions

5.1 Discussion

In this thesis, I present a chronic ABM of muscle regeneration in the *mdx* mouse. Through modifications to an acute injury model of DMD published by Virgilio, the new model presented here combined the strengths of other previously developed models by Martin et al., Jarrah et al., and Houston et al., in a more comprehensive simulation of chronic injury, cellular interactions, inflammatory cues, and muscle repair. New dystrophic conditions were defined by literature-

derived rules and various damage protocols were tested to produce a model of disease progression in the *mdx* mouse and provide new insight into the cellular interactions involved in dystrophic muscle degeneration.

One key finding from the simulations was that sustained, repetitive injury, even as low as 0.25% of the muscle fibers, resulted in impaired regeneration, with decreased CSA and increased fibrosis seen in each simulation. This suggests that this amount of damage is not viable over time and implies that the amount of damage likely decreases before it can reach the linear decline seen after 2 months at 1% damage and after 6 months at the lower levels of damage, possibly through protective measures, such as increased stiffness to minimize strain or through altered cellular mechanisms that were not included within this model. As the mdx mouse fiber CSA declined to a lesser extent in response to repetitive injury than the healthy mouse, it is possible that some of the dystrophic changes, such as excess deposition of collagen, can be protective of muscle decline. Prior research has shown that the *mdx* mouse shows robust regeneration and protection from damage after the early, widespread damage in the first few weeks, causing a less severe disease phenotype than in DMD patients [26]. Both healthy and mdx mouse simulations were inflicted with the same damage protocols, therefore any differences between healthy and *mdx* are due to emergent behaviors based on the altered cell behaviors and growth factor and chemokine secretions. These simulations exploring change in damage can also help elucidate reasons behind the different disease progression found in different muscles. While muscles of the lower limb do not degenerate to the degree of patients living with DMD, the *mdx* diaphragm follows a more severe disease phenotype that is comparable to humans [28]. One possibility for the severity of the diaphragm disease progression is that although it experiences lower strains

than the lower limb muscle, it is used more often, causing more frequent contraction-induced damage. In addition to the daily inflicted damage, 1% damage every 3 days was simulated. This was found to prevent a switch from a pro-inflammatory to anti-inflammatory environment, which likely contributed to the impaired regeneration shown in the simulation [48]. These results suggest that injury at any point while the muscle is still recovering can have devastating affects due to the simultaneous presence of inflammatory and anti-inflammatory microenvironment. Simulations of longer time in between injuries also demonstrated that while overuse may contribute to the increased severity, disease progression is much more complex than that, with many other contributing behaviors from cells, such as SSCs, fibroblasts, and inflammatory cells that are all affected by the lack of dystrophin.

Cellular interactions are difficult to recapitulate in a model and many physiological parameters are unknown. This uncertainty emphasizes the importance of computational modeling to guide future experiments. SSC recruitment and activation were parameters that Virgilio et al. and Martin et al. both struggled to address [7,8]. Martin et al. used HGF to recruit SSCs to the environment but noted that this value declined quickly as damage was cleared. Virgilio et al. altered this value so that SSCs were dependent on the recent damage signal, which decayed slowly to allow for prolonged recruitment in comparison to HGF. This model explored another possible recruitment method that was similar to Martin et al. in that recruitment was based on HGF, but in addition FGF and IGF secretion influenced recruitment [44,45]. Like Martin et al., this model did not recruit enough SSCs, even with the addition of other growth factors. One attempt to mitigate the low SSC numbers in the model was scaling the HGF based on the number of fibers, however this did not change the SSC counts, suggesting that another factor is

contributing to the lower number of SSCs. Another possibility is to explore the SSC and fibroblast interactions further, as changing fibroblast recruitment has been shown to impact SSC recruitment [18]. Future iterations should explore SSC activation and division to better understand the SSC dynamics and what is missing within the model.

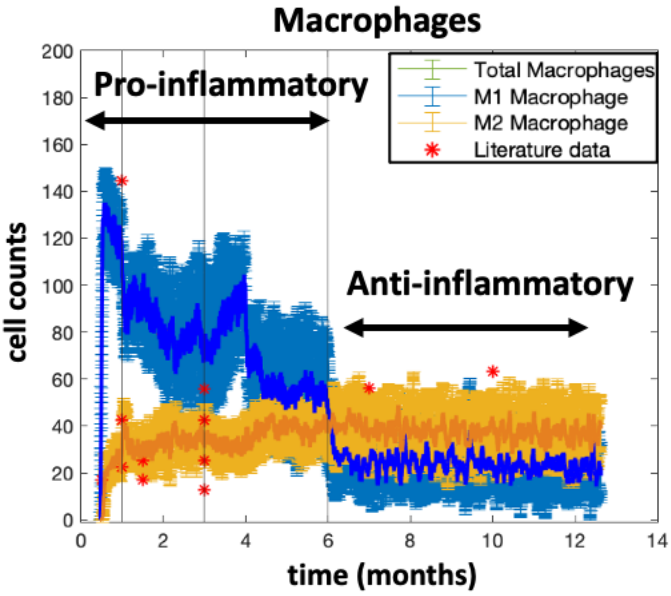

Figure 5.1. Transition from a pro-inflammatory to anti-inflammatory environment after 6 months. In the variable damage simulation that was meant to represent an *mdx* mouse, the model environment switched from primarily M1 pro-inflammatory macrophages to primarily M2 anti-inflammatory macrophages.

Another emergent behavior revealed in the variable damage model was the switch from a pro-inflammatory environment to any anti-inflammatory, pro-fibrotic environment at 6 months old. This transition from a pro- to anti-inflammatory environment is supported by the literature, which asserts that as the *mdx* mouse ages, it transitions to a more pro-fibrotic phenotype [29]. It is validating that the model captures this transition well. However, the model exaggerates the muscle decline in later stages of the disease, suggesting that the model is missing important factors to fully represent the anti-inflammatory, profibrotic environment as this stage.

Another addition to the field was the transition of a global, non-spatial chemokine into a spatially diffused chemokine in the environment, while leaving the remaining global growth factors unchanged. This novel framework can be used to combine spatial and ODE diffusion, allowing for a mix of simple and complex secretions in future iterations. Iterations could include inflammatory and anti-inflammatory spatial cytokines to further distinguish pro-inflammatory and anti-inflammatory regions and guide cell migration. The addition of spatial cues without compromising simplified global calculations is an important feature for tuning models to the necessary complexity.

In conclusion, this chronic injury model demonstrates the complexity of disease progression and demonstrates that no single factor can perfectly predict the outcome of dystrophic muscle degeneration. The model also could be further improved, particularly within the healthy mouse simulations, which should not decline as quickly as they do.

5.2 Limitations

While this model has provided new insights into skeletal muscle degeneration caused by chronic injuries, there are several limitations that should be noted, and if possible, addressed in future iterations. First, in developing the model, I used a previously published acute injury model developed by Virgilio et al. as a foundation from which to build [7]. The same cell types and growth factors that were included in the model by Virgilio et al. were included in my developed model. This meant that other important aspects to muscle regeneration in DMD, such as the microvascular network, fatty infiltration, collagen alignment in the ECM, fiber types, dystrophin loss, and muscle contractions, were not included. Any effects of these un-modeled

parameters cannot be directly perturbed and only speculations on how they affect cell behavior or growth factors can be considered. Additionally, the parameters were developed in an acute injury model and then assumed they can be applied to low level, chronic injuries, which may not elicit the same response.

When modifying the model, I first focused on matching the macrophages and neutrophil cell counts after acute injury with the model by Virgilio et al. In transitioning from ODE inflammatory cells to spatial agents, I used an ABM by Martin et al. to initially set up macrophage and neutrophil recruitment, migration, and apoptosis; however, different normalization factors were used and not all the growth factors used in the model by Martin et al. are used in that of Virgilio et al. Additionally, in Virgilio et al. the spatial component of the growth factors was lost. Therefore, it was not a direct translation. M1 macrophage and neutrophil counts had to be increased in comparison to cell counts in Virgilio et al. to fully clear the debris in a timely manner. This increase in inflammatory cell counts could have also caused unforeseen downstream effects on the growth factors and other cell types, that might not have been recognized in the acute injury validation.

After I made the modifications discussed in Chapter 3, the model did not align with the acute injury results of M2 macrophage, SSC, or fibroblast counts. There is no published literature data (at the time of writing this thesis) that provides cell counts for acute injury in a 4 week-old *mdx* mouse, therefore an experiment should be run to collect this data for validation and tuning the model. Additionally, the model does not capture healthy muscle response to injury as well as it captures that of the *mdx* mouse, particularly at older ages, suggesting that important age-related parameters are missing in the model. Previous studies have shown that physiological

activities of both immune cells and SSCs decline with advancing age and contribute to the development of sarcopenia [1]. SSC division is decreased with subsequent divisions in the model to represent reduced regenerative capacity over time, however this parameter could be refined through a parameter sweep to better match the decline in SSC with age. In aging, chronic low-grade inflammation occurs, possibly due to lower neutrophil counts [60] and decreased phagocytosis [61], which then causes lower macrophages recruitment. Thus, rules involving inflammatory cells and SSC could be modified and tested.

Another key limitation is the lack of comprehensive data available for an entire year of the *mdx* mouse life. Thus, validation data was taken from many different published papers that measured fibrosis, collagen amount, macrophage counts, fibroblast counts, and SSC counts in the diaphragm, tibialis anterior, extensor digitorum longus, and quadriceps [23,41,51-59]. Due to this, there is widespread variation in the validation data, even after normalization, making it difficult to decide what values are best to compare the model. However, this is part of what makes development of a computational model important. The computational model can provide insight into what happens in between experimental time points and why there might be conflicting reported results.

Additionally, working with a model built by someone else can lead to simple mistakes due to misunderstanding parameters or decisions within the model. For example, I once mistook a parameter as chance asymmetric, because it was commented that this parameter represented the chance of asymmetric division. While the parameter did represent the chance of asymmetric division, the actual parameter was the opposite – chance of *symmetric* division (labeled chanceSymmetric, but I had missed the lack of an “a”). In addition., normalization of cell counts

to literature data was not well documented, and thus, difficult to decipher. This is an example of a mistake that was fixed - however, it demonstrates that there are nuanced parameters that could be understood differently between different users and that it is difficult to fully understand all of the decisions made in a complex model developed by someone else.

Another addition to the model was spatially located MCP-1, a chemokine important in macrophage migration. MCP-1 was secreted neutrophils, SSCs, and fibroblasts and then diffused using the ValueLayerDiffuser in Repast Simphony. This diffusion is calculated to evaporate some amount and diffuse the rest into the neighboring grid elements at each time step. However, chemokine diffusion is affected by complex physical and biological factors, such as interaction and binding with the ECM, that is overlooked in the model's diffusion of MCP [62]. Future iterations could alter diffusion based on ECM components and collagen density to be more accurate if needed.

Another limitation was the size of the model. A cross section of approximately 50 fibers was modeled, whereas in the soleus of a mouse there is about 900 fibers at the muscle belly [63]. Throughout the simulations, the edge fibers were more effected by repetitive damage than the middle fibers, possibly due to the easier migration of cell agents to these fibers. With more fibers, this would be less of an issue because there would be a smaller proportion of outer fibers. Additionally, a whole muscle cross section would allow for the possible inclusion of the perimysium and epimysium, which has a different collagen profile than the endomysium in the model now [64]. The inclusion of these different connective tissue types surrounding the muscle fibers and fascicles could affect the outer muscle fiber degeneration, but as the model is limited to only 50 muscle fibers, this not something we can test.

Another limitation is the large computational cost of the model. Each one-year simulation takes approximately 3 hours to run, making it difficult to iterate and troubleshoot changes. One change that could help the model to run faster would be to iterate over a larger timestep. The model iterates every 1 hour, but a sensitivity analysis could be run to determine if the time step could be increased without losing important information. The computation cost of the model should also be considered when adding new parameters discussed in the future directions, and a balance must be found between keeping the model as simple as possible, but complex enough to answer the biological question being asked.

5.3 Future directions

Inform drug treatments and exercise regimens

This model could also prove useful in testing new therapeutics and combinations of treatments. Despite some progress in therapies that target the dystrophin protein at the gene level, corticosteroid treatment is the current standard for treatment of DMD [6,32]. Incorporating corticosteroid treatment into the model could provide insight on dosing and interactions with other treatments. Corticosteroids target inflammation in the muscle, so changes within the inflammatory cell behaviors and secretions based on literature-derived rules could help better understand the how corticosteroids are most effective. Additionally, treatments targeting fibrosis or SSCs would be interesting to probe in the model. This could include drugs such as Losartan, Halofuginone, or Tamoxifen that target fibrosis or injection of SSCs at a certain timepoint [6]. Combinations of these drugs could be tested in the model to see

if they have a synergistic effect improving regeneration, which could then inform future animal experiments and clinical trials.

Another emergent behavior the ABM exhibited was initial hypertrophy for the first few months following the onset of damage. Although the simulations were not created to simulate hypertrophy following exercise, the model's emergent hypertrophy in the healthy mouse support the claim that exercise causes microinjuries that allow muscle to recover and hypertrophy, and that exercise exacerbates the dystrophic disease progression [53,65,66]. Future iterations of the model could investigate hypertrophy and overuse due to microinjuries that are caused by exercise. This could provide insight into optimal, personalized prescribed exercise regimens, considering prior injury or disease states.

Coupled ABM and micromechanical model

Another improvement to the model would be to couple the ABM with a micromechanical model of fiber strains. This was done in previous versions of the model using NetLogo and Postview [67], however an updated version of the micromechanical model was developed in FEBio. This updated model uses histology images of mouse muscle fibers to initialize the FE model and calculates the strains throughout the muscle section. These strain calculations can be used to predict location of damage in the sections, and these predictions can define where damage is occurring in the ABM. Currently in the ABM, the damage is placed randomly throughout the muscle section, so the coupled ABM-FEBio model would provide a more physiological damage prescription to the model. The coupled model would also allow for direct manipulation of dystrophin in the muscle section, and therefore would allow the model to predict outcomes of

gene therapy. Further, this would help to differentiate the healthy and *mdx* mouse, and directly compare how the muscles are damaged due to the same activity level.

Additionally, alongside developing the ABM, I have worked on a collaborative project to stain and image injured and healthy muscle sections with Procion Orange to detect damaged fibers and laminin to detect fiber sizes and locations (Fig 5.1). Muscles were damaged through a gait protocol or through various levels of eccentric contraction (10%, 20%, 30%) and then they were snap frozen, sectioned, stained, and imaged using a confocal microscope. The immunohistochemistry images which I have collected can be used to validate the micromechanical model predictions of damage locations with the muscle fibers.

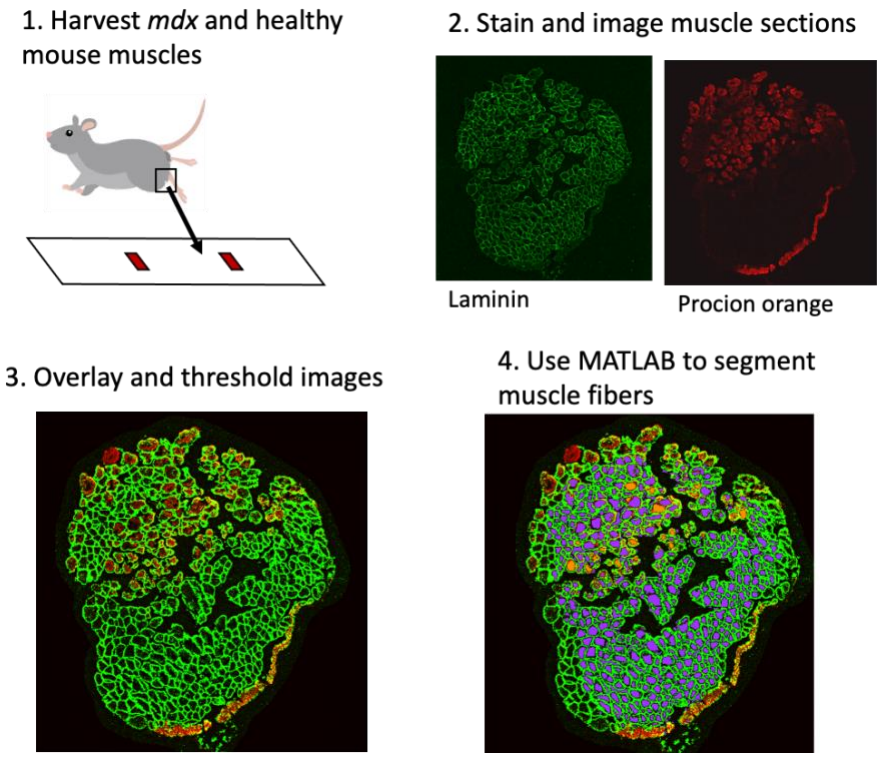

Figure 5.2 Mouse muscle histology. *mdx* mouse muscle were obtained from collaborators at Virginia Tech. I then had them sectioned, and I stained and imaged for Procion orange and Laminin. I overlayed and threslolded the images before sending them to another student for segmentation analysis in MATLAB.

Transition to a human model

The *mdx* model does not exhibit as severe of a dystrophic phenotype as that observed in boys with DMD, highlighting the need for a human-specific model [28]. Despite extensive research and knowing the cause of DMD, there is no cure for DMD and current treatments have had limited efficacy because promising treatments in mice do not translate to clinical benefit in patients [6]. Recently, Rooney et al. published a longitudinal 6-year study of MRI and magnetic resonance spectroscopy (MRS) from 104 individuals with DMD and 51 healthy controls [68]. This data could be used to inform machine learning methods in order to transform the previously developed ABM of dystrophic mouse muscle into an ABM of human dystrophic muscle. First, a longitudinal 6-year study of MRI and magnetic resonance spectroscopy (MRS) from 104 individuals with DMD and 51 healthy controls should be split into two groups, one of which will be used to train a machine learning algorithm of DMD disease progression in humans, while the second will be saved for validation. Then, a parameter sweep should be run of the refined mdx mouse ABM varying initial conditions and parameters to represent literature-based physiologic ranges of cell and cytokine levels in human dystrophic muscle. Using the machine learning algorithm to analyze outputs from the ABM parameter sweep, the set of ABM parameters that best predict the disease progression in DMD patients could be determined. Predictions of fiber CSA changes, chronic inflammation, necrosis, and fibrosis determined by this new set of ABM parameters could be validated against the MRI and MRS data not used for training previously.

Understanding differences between the *mdx* mouse model and DMD patients is essential in elucidating the reasons for failed clinical translation of treatments that were successful in mice and the coupling of ABMs with machine learning approaches could help to reveal key differences.

In conclusion, there are many options to continue the work presented in this thesis to address the need for a deeper understanding of chronic injuries, disease progression, and treatment of muscular dystrophy.

References

1. Domingues-Faria C, Vasson MP, Goncalves-Mendes N, Boirie Y, Walrand S. Skeletal muscle regeneration and impact of aging and nutrition. Ageing Research Reviews. 2016 Mar;26:22-36. DOI: 10.1016/j.arr.2015.12.004.
2. Ervasti JM, Ohlendieck K, Kahl SD, Gaver MG, Campbell KP. Deficiency of a glycoprotein component of the dystrophin complex in dystrophic muscle. Nature. 1990 May 24;345(6273):315-9. doi: 10.1038/345315a0. PMID: 2188135.
3. De Paepe B, De Bleecker JL. Cytokines and chemokines as regulators of skeletal muscle inflammation: presenting the case of Duchenne muscular dystrophy. Mediators Inflamm. 2013;2013:540370. doi: 10.1155/2013/540370. Epub 2013 Nov 5. PMID: 24302815; PMCID: PMC3835490.
4. Deconinck N, Dan B. Pathophysiology of duchenne muscular dystrophy: current hypotheses. Pediatr Neurol. 2007 Jan;36(1):1-7. doi: 10.1016/j.pediatrneurol.2006.09.016. PMID: 17162189.
5. Emery AE. Population frequencies of inherited neuromuscular diseases--a world survey. *Neuromuscul Disord*. 1991;1(1):19-29. doi:10.1016/0960-8966(91)90039-u
6. Guiraud S, Davies KE. Pharmacological advances for treatment in Duchenne muscular dystrophy. Curr Opin Pharmacol. 2017 Jun;34:36-48. doi: 10.1016/j.coph.2017.04.002. Epub 2017 May 6. PMID: 28486179.
7. Virgilio KM, Martin KS, Peirce SM, Blemker SS. Agent-based model illustrates the role of the microenvironment in regeneration in healthy and mdx skeletal muscle. J Appl Physiol (1985). 2018 Nov 1;125(5):1424-1439. doi: 10.1152/japplphysiol.00379.2018. Epub 2018 Aug 2. PMID: 30070607; PMCID: PMC6295486.
8. Martin KS, Virgilio KM, Peirce SM, Blemker SS. Computational Modeling of Muscle Regeneration and Adaptation to Advance Muscle Tissue Regeneration Strategies. Cells Tissues Organs. 2016;202(3-4):250-266. doi: 10.1159/000443635. Epub 2016 Nov 9. PMID: 27825162.
9. Jarrah AS, Castiglione F, Evans NP, Grange RW, Laubenbacher R. A mathematical model of skeletal muscle disease and immune response in the mdx mouse. Biomed Res Int. 2014;2014:871810. doi: 10.1155/2014/871810. Epub 2014 Jun 11. PMID: 25013809; PMCID: PMC4071953.
10. Houston MT, Gutierrez JB. The FRiND Model: A Mathematical Model for Representing Macrophage Plasticity in Muscular Dystrophy Pathogenesis. Bull Math Biol. 2019 Oct;81(10):3976-3997. doi: 10.1007/s11538-019-00635-8. Epub 2019 Jul 13. PMID: 31302876; PMCID: PMC6764940.
11. Westman AM, Peirce SM, Christ GJ, Blemker SS (2021) Agent-based model provides insight into the mechanisms behind failed regeneration following volumetric muscle loss injury. PLOS Computational Biology 17(5): e1008937. https://doi.org/10.1371/journal.pcbi.1008937
12. Domingues-Faria C, Vasson MP, Goncalves-Mendes N, Boirie Y, Walrand S. Skeletal muscle regeneration and impact of aging and nutrition. Ageing Res Rev. 2016 Mar;26:22-36. doi: 10.1016/j.arr.2015.12.004. Epub 2015 Dec 9. PMID: 26690801.

13. Tidball JG. Regulation of muscle growth and regeneration by the immune system. Nat Rev Immunol. 2017 Mar;17(3):165-178. doi: 10.1038/nri.2016.150. Epub 2017 Feb 6. PMID: 28163303; PMCID: PMC5452982.
14. Dumont, N., Wang, Y., von Maltzahn, J. *et al.* Dystrophin expression in muscle stem cells regulates their polarity and asymmetric division. *Nat Med* 21, 1455–1463 (2015). https://doi.org/10.1038/nm.3990
15. Yin H, Price F, Rudnicki MA. Satellite cells and the muscle stem cell niche. Physiol Rev. 2013 Jan;93(1):23-67. doi: 10.1152/physrev.00043.2011. PMID: 23303905; PMCID: PMC4073943.
16. Contreras O, Rebolledo DL, Oyarzún JE, Olguín HC, Brandan E. Connective tissue cells expressing fibro/adipogenic progenitor markers increase under chronic damage: relevance in fibroblast-myofibroblast differentiation and skeletal muscle fibrosis. Cell Tissue Res. 2016 Jun;364(3):647-660. doi: 10.1007/s00441-015-2343-0. Epub 2016 Jan 7. PMID: 26742767.
17. Biferali B, Proietti D, Mozzetta C, Madaro L. Fibro-Adipogenic Progenitors Cross-Talk in Skeletal Muscle: The Social Network. Front Physiol. 2019 Aug 21;10:1074. doi: 10.3389/fphys.2019.01074. PMID: 31496956; PMCID: PMC6713247.
18. Murphy MM, Lawson JA, Mathew SJ, Hutcheson DA, Kardon G. Satellite cells, connective tissue fibroblasts and their interactions are crucial for muscle regeneration. Development. 2011 Sep;138(17):3625-37. doi: 10.1242/dev.064162. PMID: 21828091; PMCID: PMC3152921.
19. Lemos, D., Babaeijandaghi, F., Low, M. *et al.* Nilotinib reduces muscle fibrosis in chronic muscle injury by promoting TNF-mediated apoptosis of fibro/adipogenic progenitors.*Nat Med* 21, 786–794 (2015). https://doi.org/10.1038/nm.3869
20. Petrof BJ, Shrager JB, Stedman HH, Kelly AM, Sweeney HL. Dystrophin protects the sarcolemma from stresses developed during muscle contraction. Proc Natl Acad Sci U S A. 1993 Apr 15;90(8):3710-4. doi: 10.1073/pnas.90.8.3710. PMID: 8475120; PMCID: PMC46371.
21. Zanotti, S., Gibertini, S. & Mora, M. Altered production of extra-cellular matrix components by muscle-derived Duchenne muscular dystrophy fibroblasts before and after TGF-β1 treatment. *Cell Tissue Res*339, 397–410 (2010). https://doi.org/10.1007/s00441-009-0889-4
22. Mezzano V, Cabrera D, Vial C, Brandan E. Constitutively activated dystrophic muscle fibroblasts show a paradoxical response to TGF-beta and CTGF/CCN2. J Cell Commun Signal. 2007 Dec;1(3-4):205-17. doi: 10.1007/s12079-008-0018-2. Epub 2008 Apr 15. PMID: 18600480; PMCID: PMC2443238.
23. Jiang C, Wen Y, Kuroda K, Hannon K, Rudnicki MA, Kuang S. Notch signaling deficiency underlies age-dependent depletion of satellite cells in muscular dystrophy. Dis Model Mech. 2014 Aug;7(8):997-1004. doi: 10.1242/dmm.015917. Epub 2014 Jun 6. PMID: 24906372; PMCID: PMC4107328.
24. Boldrin L, Zammit PS, Morgan JE. Satellite cells from dystrophic muscle retain regenerative capacity. Stem Cell Res. 2015 Jan;14(1):20-9. doi: 10.1016/j.scr.2014.10.007. Epub 2014 Nov 1. PMID: 25460248; PMCID: PMC4305370.

25. Webster, C., Blau, H.M. Accelerated age-related decline in replicative life-span of Duchenne muscular dystrophy myoblasts: Implications for cell and gene therapy. *Somat Cell Mol Genet* 16, 557–565 (1990). https://doi.org/10.1007/BF01233096
26. Yucel, N., Chang, A.C., Day, J.W. *et al.* Humanizing the mdx mouse model of DMD: the long and the short of it. *npj Regen Med* 3, 4 (2018). https://doi.org/10.1038/s41536-018-0045-4
27. Dangain J, Vrbova G. Muscle development in mdx mutant mice. Muscle Nerve. 1984 Nov-Dec;7(9):700-4. doi: 10.1002/mus.880070903. PMID: 6543918.
28. Stedman HH, Sweeney HL, Shrager JB, Maguire HC, Panettieri RA, Petrof B, Narusawa M, Leferovich JM, Sladky JT, Kelly AM. The mdx mouse diaphragm reproduces the degenerative changes of Duchenne muscular dystrophy. Nature. 1991 Aug 8;352(6335):536-9. doi: 10.1038/352536a0. PMID: 1865908.
29. Pessina P, Cabrera D, Morales MG, Riquelme CA, Gutiérrez J, Serrano AL, Brandan E, Muñoz-Cánoves P. Novel and optimized strategies for inducing fibrosis in vivo: focus on Duchenne Muscular Dystrophy. Skelet Muscle. 2014 Aug 25;4:7. doi: 10.1186/2044-5040-4-7. PMID: 25157321; PMCID: PMC4142391.
30. Carnwath JW, Shotton DM. Muscular dystrophy in the mdx mouse: histopathology of the soleus and extensor digitorum longus muscles. J Neurol Sci. 1987 Aug;80(1):39-54. doi: 10.1016/0022-510x(87)90219-x. PMID: 3612180.
31. Lu A, Poddar M, Tang Y, Proto JD, Sohn J, Mu X, Oyster N, Wang B, Huard J. Rapid depletion of muscle progenitor cells in dystrophic mdx/utrophin-/- mice. Hum Mol Genet. 2014 Sep 15;23(18):4786-800. doi: 10.1093/hmg/ddu194. Epub 2014 Apr 29. PMID: 24781208; PMCID: PMC4140461.
32. Lim KR, Maruyama R, Yokota T. Eteplirsen in the treatment of Duchenne muscular dystrophy. Drug Des Devel Ther. 2017 Feb 28;11:533-545. doi: 10.2147/DDDT.S97635. PMID: 28280301; PMCID: PMC5338848.
33. Dadgar S, Wang Z, Johnston H, Kesari A, Nagaraju K, Chen YW, Hill DA, Partridge TA, Giri M, Freishtat RJ, Nazarian J, Xuan J, Wang Y, Hoffman EP. Asynchronous remodeling is a driver of failed regeneration in Duchenne muscular dystrophy. J Cell Biol. 2014 Oct 13;207(1):139-58. doi: 10.1083/jcb.201402079. PMID: 25313409; PMCID: PMC4195829.
34. H. E. Huxley, “The mechanism of muscular contraction.,” *Science*, vol. 164, no. 3886, pp. 1356–65, Jun. 1969.
35. F. E. Zajac, “Muscle and tendon: properties, models, scaling, and application to biomechanics and motor control.,” *Crit. Rev. Biomed. Eng.*, vol. 17, no. 4, pp. 359–411, 1989.
36. S. S. Blemker and S. L. Delp, “Rectus femoris and vastus intermedius fiber excursions predicted by three-dimensional muscle models,” *J. Biomech.*, vol. 39, no. 8, pp. 1383–1391, Jan. 2006.
37. A. Seth *et al.*, “OpenSim: Simulating musculoskeletal dynamics and neuromuscular control to study human and animal movement,” *PLOS Comput. Biol.*, vol. 14, no. 7, p. e1006223, Jul. 2018.
38. Martin KS, Blemker SS, Peirce SM. Agent-based computational model investigates muscle-specific responses to disuse-induced atrophy. J Appl Physiol (1985). 2015 May

15;118(10):1299-309. doi: 10.1152/japplphysiol.01150.2014. Epub 2015 Feb 26. PMID: 25722379; PMCID: PMC4436981.
39. Dell'Acqua G, Castiglione F. Stability and phase transitions in a mathematical model of Duchenne muscular dystrophy. J Theor Biol. 2009 Sep 21;260(2):283-9. doi: 10.1016/j.jtbi.2009.05.037. Epub 2009 Jun 11. PMID: 19523962.
40. The Jackson Laboratory. JAX Mice Pup Appearance by Age. https://oacu.oir.nih.gov/sites/default/files/uploads/training-resources/jaxpupsposter.pdf
41. Evans NP, Call JA, Bassaganya-Riera J, Robertson JL, Grange RW. Green tea extract decreases muscle pathology and NF-kappaB immunostaining in regenerating muscle fibers of mdx mice. Clin Nutr. 2010 Jun;29(3):391-8. doi: 10.1016/j.clnu.2009.10.001. Epub 2009 Nov 7. PMID: 19897286; PMCID: PMC2882522.
42. Saclier M, Cuvellier S, Magnan M, Mounier R, Chazaud B. Monocyte/macrophage interactions with myogenic precursor cells during skeletal muscle regeneration. FEBS J. 2013 Sep;280(17):4118-30. doi: 10.1111/febs.12166. Epub 2013 Feb 28. PMID: 23384231.
43. Chazaud B, Sonnet C, Lafuste P, Bassez G, Rimaniol AC, Poron F, Authier FJ, Dreyfus PA, Gherardi RK. Satellite cells attract monocytes and use macrophages as a support to escape apoptosis and enhance muscle growth. J Cell Biol. 2003 Dec 8;163(5):1133-43. doi: 10.1083/jcb.200212046. PMID: 14662751; PMCID: PMC2173611.
44. Allen RE, Boxhorn LK. Regulation of skeletal muscle satellite cell proliferation and differentiation by transforming growth factor-beta, insulin-like growth factor I, and fibroblast growth factor. J Cell Physiol. 1989 Feb;138(2):311-5. doi: 10.1002/jcp.1041380213. PMID: 2918032.
45. Doumit ME, Cook DR, Merkel RA. Fibroblast growth factor, epidermal growth factor, insulin-like growth factors, and platelet-derived growth factor-BB stimulate proliferation of clonally derived porcine myogenic satellite cells. J Cell Physiol. 1993 Nov;157(2):326-32. doi: 10.1002/jcp.1041570216. PMID: 8227164.
46. Nguyen HX, Tidball JG. Interactions between neutrophils and macrophages promote macrophage killing of rat muscle cells in vitro. J Physiol. 2003 Feb 15;547(Pt 1):125-32. doi: 10.1113/jphysiol.2002.031450. Epub 2002 Dec 20. PMID: 12562965; PMCID: PMC2342622.
47. Heredia JE, Mukundan L, Chen FM, Mueller AA, Deo RC, Locksley RM, Rando TA, Chawla A. Type 2 innate signals stimulate fibro/ adipogenic progenitors to facilitate muscle regeneration. *Cell* 153: 376– 388, 2013. doi:10.1016/j.cell.2013.02.053.
48. ArnoldL,HenryA,PoronF,Baba-AmerY,vanRooijenN,Plonquet A, Gherardi RK, Chazaud B. Inflammatory monocytes recruited after skeletal muscle injury switch into antiinflammatory macrophages to support myogenesis. *J Exp Med* 204: 1057–1069, 2007. doi:10.1084/jem. 20070075.
49. Wang YX, Dumont NA, Rudnicki MA. Muscle stem cells at a glance. *J Cell Sci* 127: 4543–4548, 2014. doi:10.1242/jcs.151209.

50. Muñoz-Cánoves P, Serrano AL. Macrophages decide between regeneration and fibrosis in muscle. Trends in Endocrinology and Metabolism: TEM. 2015 Sep;26(9):449-450. DOI: 10.1016/j.tem.2015.07.005.
51. Vidal B, Serrano AL, Tjwa M, Suelves M, Ardite E, De Mori R, Baeza-Raja B, Martínez de Lagrán M, Lafuste P, Ruiz-Bonilla V, Jardí M, Gherardi R, Christov C, Dierssen M, Carmeliet P, Degen JL, Dewerchin M, Muñoz-Cánoves P. Fibrinogen drives dystrophic muscle fibrosis via a TGFbeta/alternative macrophage activation pathway. Genes Dev. 2008 Jul 1;22(13):1747-52. doi: 10.1101/gad.465908. PMID: 18593877; PMCID: PMC2492661.
52. Virgilio, K.M., Jones, B.K., Miller, E.Y. *et al.* Computational Models Provide Insight into *In Vivo* Studies and Reveal the Complex Role of Fibrosis in *mdx* Muscle Regeneration. *Ann Biomed Eng* 49, 536–547 (2021). https://doi.org/10.1007/s10439-020-02566-1
53. Pessina P, Cabrera D, Morales MG, Riquelme CA, Gutiérrez J, Serrano AL, Brandan E, Muñoz-Cánoves P. Novel and optimized strategies for inducing fibrosis in vivo: focus on Duchenne Muscular Dystrophy. Skelet Muscle. 2014 Aug 25;4:7. doi: 10.1186/2044-5040-4-7. PMID: 25157321; PMCID: PMC4142391.
54. Villalta SA, Rinaldi C, Deng B, Liu G, Fedor B, Tidball JG. Interleukin-10 reduces the pathology of mdx muscular dystrophy by deactivating M1 macrophages and modulating macrophage phenotype. Hum Mol Genet. 2011 Feb 15;20(4):790-805. doi: 10.1093/hmg/ddq523. Epub 2010 Nov 30. PMID: 21118895; PMCID: PMC3024048.
55. Shefer G, Van de Mark DP, Richardson JB, Yablonka-Reuveni Z. Satellite-cell pool size does matter: defining the myogenic potency of aging skeletal muscle. Dev Biol. 2006 Jun 1;294(1):50-66. doi: 10.1016/j.ydbio.2006.02.022. Epub 2006 Mar 22. PMID: 16554047; PMCID: PMC2710453.
56. Farini A, Meregalli M, Belicchi M, Battistelli M, Parolini D, D'Antona G, Gavina M, Ottoboni L, Constantin G, Bottinelli R, Torrente Y. T and B lymphocyte depletion has a marked effect on the fibrosis of dystrophic skeletal muscles in the scid/mdx mouse. J Pathol. 2007 Oct;213(2):229-38. doi: 10.1002/path.2213. PMID: 17668421.
57. Duddy, W., Duguez, S., Johnston, H. *et al.* Muscular dystrophy in the *mdx* mouse is a severe myopathy compounded by hypotrophy, hypertrophy and hyperplasia. *Skeletal Muscle* 5, 16 (2015). https://doi.org/10.1186/s13395-015-0041-y
58. Sacco A, Mourkioti F, Tran R, Choi J, Llewellyn M, Kraft P, Shkreli M, Delp S, Pomerantz JH, Artandi SE, Blau HM. Short telomeres and stem cell exhaustion model Duchenne muscular dystrophy in mdx/mTR mice. Cell. 2010 Dec 23;143(7):1059-71. doi: 10.1016/j.cell.2010.11.039. Epub 2010 Dec 9. PMID: 21145579; PMCID: PMC3025608.
59. Henry CC, Martin KS, Ward BB, Handsfield GG, Peirce SM, Blemker SS. Spatial and age-related changes in the microstructure of dystrophic and healthy diaphragms. PLoS One. 2017 Sep 6;12(9):e0183853. doi: 10.1371/journal.pone.0183853. PMID: 28877195; PMCID: PMC5587283.
60. De Martinis M, Modesti M, Ginaldi L. Phenotypic and functional changes of circulating monocytes and polymorphonuclear leucocytes from elderly persons. Immunol Cell Biol. 2004 Aug;82(4):415-20. doi: 10.1111/j.0818-9641.2004.01242.x. PMID: 15283852.
61. Niwa Y, Kasama T, Miyachi Y, Kanoh T. Neutrophil chemotaxis, phagocytosis and parameters of reactive oxygen species in human aging: cross-sectional and longitudinal

studies. Life Sci. 1989;44(22):1655-64. doi: 10.1016/0024-3205(89)90482-7. PMID: 2733545.
62. Moore JE Jr, Brook BS, Nibbs RJB. Chemokine Transport Dynamics and Emerging Recognition of Their Role in Immune Function. Curr Opin Biomed Eng. 2018 Mar;5:90-95. doi: 10.1016/j.cobme.2018.03.001. Epub 2018 Mar 20. PMID: 30320240; PMCID: PMC6176735.
63. Timson BF, Bowlin BK, Dudenhoeffer GA, George JB. Fiber number, area, and composition of mouse soleus muscle following enlargement. J Appl Physiol (1985). 1985 Feb;58(2):619-24. doi: 10.1152/jappl.1985.58.2.619. PMID: 3980364.
64. Light N, Champion AE. Characterization of muscle epimysium, perimysium and endomysium collagens. Biochem J. 1984 May 1;219(3):1017-26. doi: 10.1042/bj2191017. PMID: 6743238; PMCID: PMC1153576.
65. Proske U, Morgan DL. Muscle damage from eccentric exercise: mechanism, mechanical signs, adaptation and clinical applications. J Physiol. 2001 Dec 1;537(Pt 2):333-45. doi: 10.1111/j.1469-7793.2001.00333.x. PMID: 11731568; PMCID: PMC2278966.
66. Schoenfeld BJ. Does exercise-induced muscle damage play a role in skeletal muscle hypertrophy? J Strength Cond Res. 2012 May;26(5):1441-53. doi: 10.1519/JSC.0b013e31824f207e. PMID: 22344059.
67. Virgilio KM, Martin KS, Peirce SM, Blemker SS. Multiscale models of skeletal muscle reveal the complex effects of muscular dystrophy on tissue mechanics and damage susceptibility. Interface Focus. 2015 Apr 6;5(2):20140080. doi: 10.1098/rsfs.2014.0080. PMID: 25844152; PMCID: PMC4342948.
68. Rooney WD, Berlow YA, Triplett WT, Forbes SC, Willcocks RJ, Wang DJ, Arpan I, Arora H, Senesac C, Lott DJ, Tennekoon G, Finkel R, Russman BS, Finanger EL, Chakraborty S, O'Brien E, Moloney B, Barnard A, Sweeney HL, Daniels MJ, Walter GA, Vandenborne K. Modeling disease trajectory in Duchenne muscular dystrophy. Neurology. 2020 Apr 14;94(15):e1622-e1633. doi: 10.1212/WNL.0000000000009244. Epub 2020 Mar 17. PMID: 32184340; PMCID: PMC7251517.
69. Mann CJ, Perdiguero E, Kharraz Y, Aguilar S, Pessina P, Serrano AL, Muñoz-Cánoves P. Aberrant repair and fibrosis development in skeletal muscle. Skelet Muscle. 2011 May 4;1(1):21. doi: 10.1186/2044-5040-1-21. PMID: 21798099; PMCID: PMC3156644.
70. Pratt SJP, Shah SB, Ward CW, Kerr JP, Stains JP, Lovering RM. Recovery of altered neuromuscular junction morphology and muscle function in mdx mice after injury. *Cell Mol Life Sci* 72: 153–164, 2015. doi:10.1007/s00018-014-1663-7.
71. De Rossi M, Bernasconi P, Baggi F, de Waal Malefyt R, Mantegazza R. Cytokines and chemokines are both expressed by human myoblasts: possible relevance for the immune pathogenesis of muscle inflammation. *Int Immunol* 12: 1329 –1335, 2000. doi:10.1093/intimm/12.9.1329.
72. Dickinson RB, Guido S, Tranquillo RT. Biased cell migration of fibroblasts exhibiting contact guidance in oriented collagen gels. *Ann Biomed Eng* 22: 342–356, 1994. doi:10.1007/BF02368241.